

Analysis of Impedance Measurement Implementation Using Particular Sampling (By Lab View and Matlab)

Rohith Kumar Prasanna Kumar

Abstract— The paper describes an impedance measurement technique using a particular sampling method which is a time saving and helpful method as compared to the complexity of DFT calculation. In this technique a sinusoidal signal is used as an excitation signal and the response of the signal that are proportional to current flowing through and voltage across the measured impedance got after by sampling are extracted and processed. The impedance of the object under consideration is calculated without using Fourier transform. This method will be first evaluated in MATLAB by means of simulation.

This paper is definitely a comparison of two impedance measurement methods namely the DFT and particular sampling in the domains of error, time savings and standard deviation. The Labview application is used to generate the excitation signal using the data acquisition card NI-USB 6251. The sampled responses are compared by the graphical program developed in the labview platform is used to compute the error, standard deviation and percentage of time saving.

Index Terms— Data acquisitions, Fourier transform Impedance, Matlab, Labview

LIST OF IMPORTANT SYMBOLS ABBREVIATIONS

AC	- Alternating Current
dB	- Decibels
DC	- Direct Current
DDS	- Direct Digital Synthesis
DFT	- Discrete Fourier Transformation
DSP	- Digital Signal Processing
e	- Electrons
EDF	- Electricité de France
F	- Farad
f	- Frequency
FFT	- Fast Fourier transformation
G	- Conductance
Hz	- Hertz (unit of frequency)
I	- Current
IET	- Institution of Engineering
IEEE	- Institute of Electrical and Electronic Engineers
k	- Kilo
LCR	- Inductance (L), Capacitance (C) and Resistance (R)
M	- Mega
n	- Nano
p	- Pico
PSoC	- Programmable System on Chips
S	- Siemens (mutual inductance)
SIR	- Source Impedance Ratio
SST	- Single sine technique
XC	- Reactance of Capacitance
XL	- Reactance of Inductance
R	- Resistance
Z	- Impedance
Ω	- Ohms (Unit of reactance)
ω	- Angular frequency
ϕ	- Phase angle

Rohith Kumar Prasanna Kumar, Msc Electronics and Telecommunications, Gdansk University of Technology, Poland, University ID : S164408

I. INTRODUCTION

The terms impedance and resistance both means oppose to the flow of current. In circuits working on direct current, only resistors produce this effect. On the other hand in alternating current (ac) circuits, the other components, like inductors and capacitors, also provides opposition to the flow of current. The total impedance in a circuit is the sum of opposition of all the elements to the flow of current. The opposition provided by inductors and capacitors in a circuit is called by the same name reactance, characterized by X and calculated in ohms (Ω). Since the symbol for capacitance is C, capacitive reactance is represented by XC. Similarly, since the symbol for inductance is L, reactance offered by inductance is represented by XL. Inductors and capacitors not only affect the magnitude of an alternating current but also its time dependent properties – or phase. When most of reactance to current flow in a circuit is offered by a capacitor, a circuit is said to be largely capacitive and the current through the circuit is said to be leading the voltage in phase angle. When most of the reactance to the current flowing through the circuit comes from an inductor, a circuit is said to be largely inductive and the current is said to be lagging behind, the applied voltage in phase angle. The more inductive a circuit is, the phase difference between the current and voltage approaches 90 degrees. It's sometimes easier to perform calculations using admittance, the mutual impedance. Admittance is characterized by Y and calculated in Siemens (S). Like impedance, admittance can be explicate as a intricate figure, where the conductance, the mutual of resistance, is the real item, and the susceptance, the mutual of reactance, is the imaginary item.

There are numerous specialized and organic objects, the parameters of which can be evaluated by impedance estimation. A case of such approach is checking and diagnostics of anticorrosion protection of huge specialized items like pipelines, extensions, fuel tanks and so on. A case of natural security and wellbeing is the utilization of impedance estimation for observing of water permeation of dams. Another illustration is detecting innovation e.g. relative humidity sensors. In the event of the initial two cases there is a need of circulated estimations in numerous spots – various sensors are required, so the estimation time is expanded definitively or the required number of instruments working in parallel gets to be higher. If there should be an occurrence of sensors, the aggregate cost of the gadget, circuit measurements and power utilization ought to be kept as little as would be prudent for the most part because of monetary reasons. The above displayed rules prompt scanning for new strategies which permit to disentangle impedance estimation instrument.

Local impedance calculation methods are always revised because of highly effective digital and analog converters development, making use of the digital signal processing methods and fast construction of recent and more energized digital executing signals which can effectively undergo a lot of operations in each second. Measurement of impedance is a very essential subject with various recent findings researched newly. Few research works have been targeted on measurement of the impedance sensors while some utilize the newly transmitted network executing algorithms to enhance impedance calculation. An easy impedance calculation technique staged and improved minimized the front-end analog circuit to diminish the effect of frequency dependence. This method is staged with volt-ampere method with anonymous impedance and reference impedance arranged in series and delivered with same electric current from a sine generator. Voltage across each impedance is acquired simultaneously with dual analog to digital channel converter with the phase of impedance extracted with aid of signal processing digital algorithm.

Algorithms with sine-fit structure have an option to calculate the signal parameters [15] within a group of acquired samples. Ever since gap within the sampling rate and sine wave frequency mostly are not known by accuracy, the said algorithm should be able to calculate sine wave frequency as well. It allows the issue of regression of nonlinear which is sorted by using procedure of iterative that is named sine-fit four parameters algorithm. Take for instance the measurements for impedance, the structure algorithm may be used on the channels individually, moreover the final researched probability may be diminished by moving the common rate of occurrence with force in a seven sine-fit parameter algorithm [15]. Nevertheless, the iterative impedance structure of the sine fit output large amount of processes that must be executed. Another problem that may hinder effectiveness of the algorithm developed with device such as DSP is memory management and specifications. It should be noted that the seven sine-fit algorithm developed 2N rows and seven column matrix, in accordance to the sum of acquired samples by both channels.

This large matrix and its manipulation together with the limited memory available in the DSP restrict the number of samples that can be processed. In this paper, the algorithm proposed is shown to be applicable in a memory restricted system by bypassing the need to build the 2N*7 matrix. This modification allows DSP to process more samples to calculate the sine wave frequency that must be accurately known for a correct calculation of the sine signals' amplitudes, phases and DC items by the sine-fit algorithm [15], in impedance measurements an accurate frequency value is not required. The time information, and thus the sine signals frequency can be removed from the problem by making an XY plot of the two waves. The result is an ellipse whose values can be calculated by ellipse-fit algorithm such as the one presented and then improved. The sine signals values can then be extracted from the ellipse parameter as proposed. This algorithm has been recently optimized and adapted for use in DSP based impedance measurements. In the modified ellipse-fit method published [15], there is no limit on the number of samples that can be used since only nine values must be stored and the samples themselves can be discarded after their contribution to the nine stored values is taken into account. These properties make the algorithm a prime

candidate for efficient in a DSP based impedance measurement instrument.

The aim of this master diploma thesis is to present and implement impedance measurement method using particular sampling method [13], which is a substitute for DFT calculation. The method uses sine excitation signal and sampling response signal proportional to current and voltage, flowing through and across the measured impedance. Fourier transform is not used in this method. The method will be first assessed in MATLAB by means of simulation. The excitation signal is generated using National Instruments data card and graphical software platform LABVIEW. The software is developed to measure the voltage across the measured impedance and current flowing through it and hence calculate the impedance and verify it with the conventional DFT method.

The second chapter describes various methods of impedance measurements such as null method using different kinds of bench and also different meters workings on the basis of resonance method and active method. The third chapter deals with the theoretical aspects like phase-sensitive detection, DFT, FFT, sine-fit and ellipse-fit algorithm and Goertzel's algorithm, and detailed explanation of complexity of each method..

The next chapter explains the concept of particular sampling and also explains the result of simulation using MATLAB and the implementation of software part for the impedance measurement using LABVIEW for the particular sampling method. This chapter deals with the experimental data analysis on a circuit and trying to find the impedance using DFT as well as particular sampling method and determining the error in impedance measurement The next chapter describes the experimental results of the software based implementation of the particular sampling method. The next chapter includes the results based on the experimental results and scope of improving the results and thus reducing the complexity, the chapter also deals with, what have been done in the field of diploma thesis. The document is finished with bibliography section and list of figures and tables.

II. IMPEDANCE MEASUREMENT METHODS

The common methods used for impedance measurements are: auto balancing bridge method, resonant method, network analysis method. [20].

The impedance is used to specialize electronic circuits and items. At given frequency when it is passed through electronic device or circuit impedance is defined as opposition to AC (alternating current)

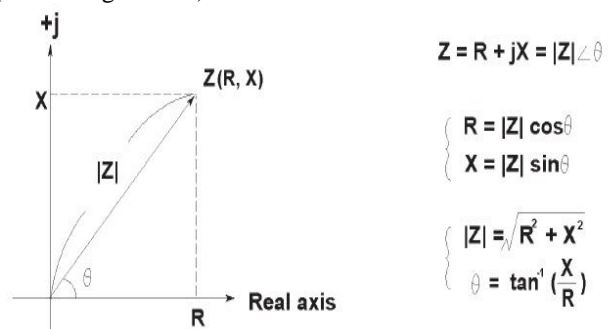


Fig. 2.1. Impedance vector analysis [10].

Fig. 2.1 shows that the impedance has an imaginary reactance X and real part resistance R. In order to measure impedance,

two values are required to be calculated as it is a complex quantity. Both real part and imaginary part of impedance vector are usually used while measuring all the impedance measurement instruments. Parameters such as $|Z|$, θ , $|Y|$, R , X , G , B , C and L , later on instrument converts these real and imaginary parts.

There are various impedance measurement methods based on various parameters, such as measurement range, frequency of operation, ease of use and measurement accuracy. The impedance measurement methods like resonant method, bridge method, I-V method, auto balancing bridge method and active methods are explained in the following sections with their advantages and disadvantages. As the recent developments in impedance measurement devices LCR meters are more commonly used for the accurate computation of impedance

In order to measure impedance, the single sine technique (SST) is commonly used. By repeating the measurements at various frequencies, the impedance spectrum can be obtained directly from measurement results as a function of frequency in a range of a few decades. SST is based on excitation of the object with a harmonic signal and vector measurement of two signals: voltage across and current through the tested object.

In the digital implementation of the impedance measurement method excitation signal is produced with the aid of Direct Digital Synthesis (DDS) using a D/A converter and memory containing sine samples. To extract signals proportional to the voltage across ($V_y - V_x$) and current through ($I_x - I_y$) the calculated impedance Z the input circuitry has to be used. The block diagram of an impedance measurement system is shown in Fig. 2.2. The construction of the input circuit is very important as parasitic capacitances and real-life parameters of the operational amplifiers can significantly influence a measurement result. Signals are sampled synchronously with the clock generator using two A/D converters and placed in memory in the form of two sets of N samples of signals, $V_y[n]$ and $V_x[n]$

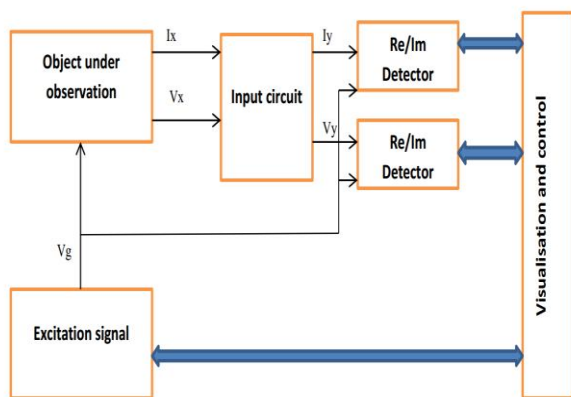


Fig. 2.2. Block diagram of the impedance measurement system.

To determine the orthogonal parts of the acquired signals on the basis of the collected samples, various techniques can be used: the use of Fourier transformation (DFT or FFT), sine-fitting algorithms, ellipse-fitting algorithms and others.

The methods of computing impedance describe the standard ways of computing impedance in the electric circuit using the concepts such as

- Null method
- Resonant method
- Active method

The strength and weakness of each measurement method depend on accuracy, cost and effectiveness. Sometimes more than one method is used to compute the impedance in the electric circuit which is dependent on the characteristics of the circuit

2.1. Null method

The principle of null method is the Wheatstone's bridge and all instruments will have an appearance as the same. The voltage is applied on one of the portion of circuit and the parameters of the circuit are adjusted to obtain the balancing condition and at this moment there exist a mathematical relation between the known and unknown components in the circuit and by which the unknown impedance can be calculated

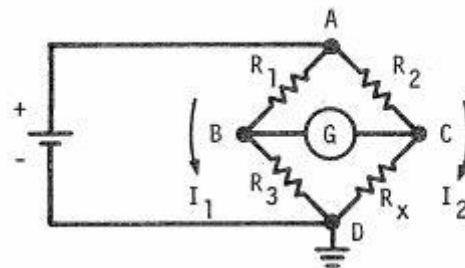


Fig. 2.3. Wheatstone's bridge [1]

Fig. 2.3. represents a Wheatstone's bridge. In the circuit diagram R_x is connected to the unknown terminals and the resistance R_1 , R_2 , R_3 is connected to the known terminals. The resistance connected in the known terminals can be adjusted to achieve the balanced condition so the galvanometer (G) connected shows the null deflection and thus the nodes B and C are at same potential.

In the balanced condition we have the following mathematical equation [1]

$$\frac{R_3}{R_x} = \frac{R_1}{R_2} \quad (2.1)$$

So we have

$$R_x = \frac{R_2}{R_1} * R_3 \quad (2.2)$$

Thus the unknown impedance can be calculated from the above equation (2.2). For the ac circuits the resistances are replaced by admittances or impedance, battery by a signal generator and the galvanometer by an ac voltage detector.

The major advantages of the null method are the accuracy of the measurement. The accuracy is dependent on the factors like dial resolution, internal shielding and constructional factors. Most null detectors are dependent on signal frequency and are designed to operate with high accuracy at an ambient frequency, below this frequency the accuracy is decreased due to the sensitivity and above this frequency the accuracy is diminished due to the residual impedance.

The different kinds of null instruments are illustrated below

- Maxwell's bridge

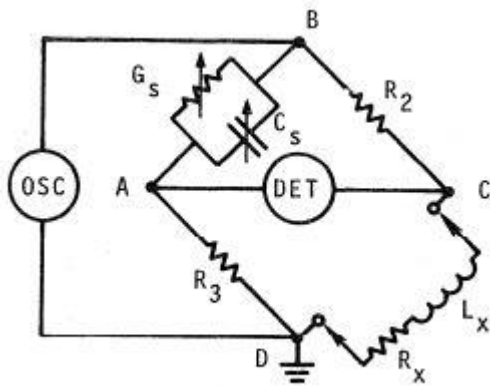


Fig. 2.4. Maxwell's bridge [1]

Fig. 2.4. shows the Maxwell's bridge, the balancing equations [1] are as follows,

$$R_x = R_2 * R_3 * \Delta G_s \tag{2.3}$$

$$L_x = R_2 * R_3 * \Delta C_s \tag{2.4}$$

Where R_x and L_x are the unknown resistance and inductance. This bridge measures the inductance and resistance connected series in terms of standard capacitance (C_s) and conductance standard (G_s). This bridge is ideal for measuring low impedance at high frequencies. The initial balance is achieved respect to the short circuit placed at the unknown terminal.

Advantages

- High accuracy
- Best among other instruments to measure very low values of impedance and series resistance.
- Broad measuring range of resistance

Disadvantages

- Maximum frequency limit is 30MHz
- Difficult to calibrate
- Slow

➤ Schering bridge

The Schering bridge is also called radio arm bridge, and is shown in Fig. 2.5. It is specialized to perform more specific measurements in one form or another and is widely used in RF bridge circuits.

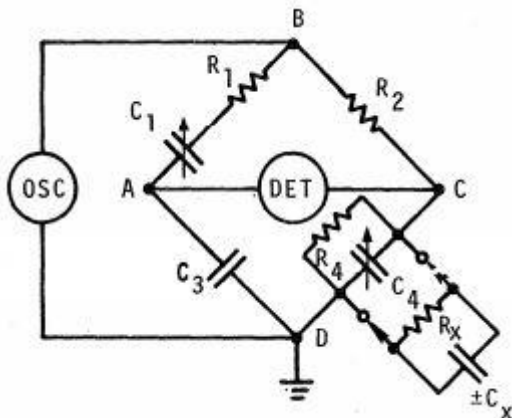


Fig. 2.5. Schering bridge [1]

The balancing equations [1] are as follows

$$\frac{R_1}{C_4} = \frac{R_2}{C_3} = \frac{R_4}{C_1} \tag{2.5}$$

$$R_x = \frac{R_2}{C_3} * \Delta C_1 \tag{2.6}$$

$$C_x = \Delta C_4 \tag{2.7}$$

R_x and C_x are the unknown resistance and capacitance. This bridge measure admittance in terms of parallel resistance equivalent and either positive or negative equivalent parallel capacitance or thus both capacitive and inductive impedance can be measured. Initially the balancing condition is achieved with respect to an open circuit and first order errors due to signal generator are not present.

Advantages

- Broad frequency range
- Less calculations needed
- Broad range of resistance value measurement
- Good accuracy

Disadvantages

- Minimum value of frequency is 500kHz
- Operator training required
- Small range of inductance and capacitance measurement
- Slow

➤ Admittance ratio bridge

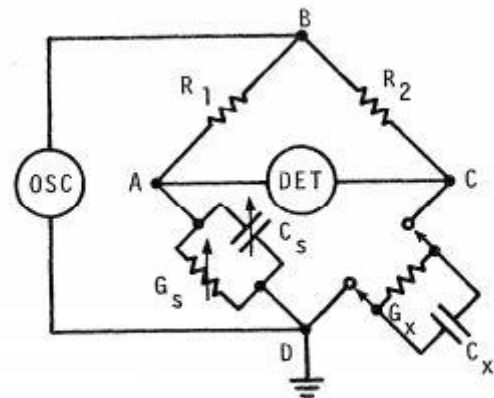


Fig. 2.6. Admittance ratio bridge [1].

Fig. 2.6. represents an admittance ratio bridge, the balance condition equations [1] is as follows,

$$G_x = \frac{R_1}{R_2} * G_s \tag{2.8}$$

$$C_x = \frac{R_1}{R_2} * C_s \tag{2.9}$$

G_x and C_x are the unknown conductance and capacitance. This bridge has its application in the low frequencies and extends up to 1 MHz. The circuit can be used as a comparator

when external standards are available. Initial balance is made with respect to an open-circuit.

Advantages

- Wide range of capacitances
- Good accuracy
- Can be used as comparator using parallel range extension

Disadvantages

- Cannot be used to measure small impedances
- Limited to frequency below 5 MHz
- Operator training needed

➤ Transformer ratio bridge

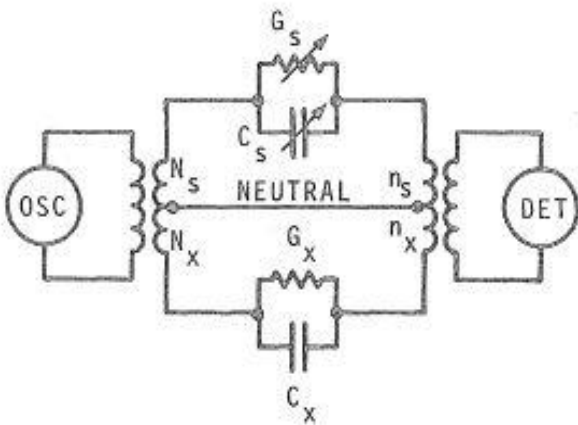


Fig. 2.7. Transformer bridge [1]

Fig. 2.7. presents the transformer bridge and the balancing condition equations [1] are,

$$G_x = \left(\frac{N_x}{N_s} * \frac{n_x}{n_s} \right) * G_s \tag{2.10}$$

$$C_x = \left(\frac{N_x}{N_s} * \frac{n_x}{n_s} \right) * C_s \tag{2.11}$$

The G_x and C_x are the unknown conductance and capacitance. This is a very special bridge that offers very wide range of measurement values than that offered by conventional Wheatstone bridge based bridges. Primary and secondary turns-ratio in in both the input and te detector positions are tapped to provide the effect of variable internal standard, thus eliminating the need of adjustable resistors and capacitors , but they can be added for higher resolutions.

Advantages

- Wide range of frequency
- Wide measurement range for resistance and inductance or capacitors
- Can be automated
- Can be made grounded, balanced or unbalanced based on measurement requirements

Disadvantages

- Very slow
- Requires skilled operator.

➤ Twin -T bridge

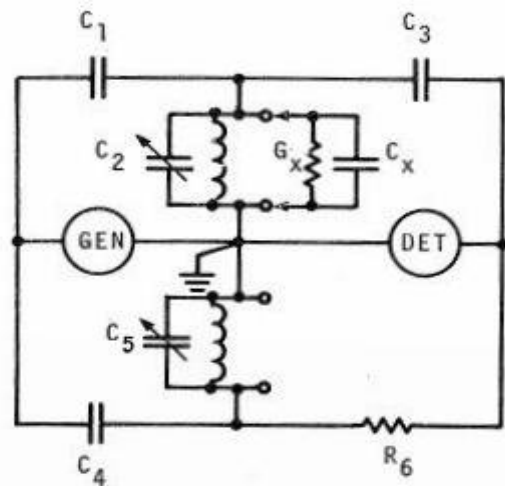


Fig. 2.8. Twin-T bridge [1]

Fig. 2.8. presents a Twin-T bridge and the balancing equations [1] are

$$G_x = \omega^2 * \left(R_6 \frac{C_1 C_3}{C_4} \right) \Delta C_5 \tag{2.12}$$

$$C_x = \Delta C_2 \tag{2.13}$$

The G_x and C_x are the unknown admittance and capacitance. The twin-t bridge is actually an admittance bridge which offers a very high accuracy. The initial balance is made by means of an open circuit and the main characteristics of the bridge is due the fact that bridge balance is frequency sensitive, represented by the factor ω^2 in the balancing equation (2.13).

Advantages

- Wide range of frequencies
- Wide range of impedances of capacitance, inductance and conductance
- Can measure conductance in terms of capacitance increment
- Most accurate method for measuring the conductance

Disadvantages

- Expensive
- Slow
- Cannot measure small resistance
- Requires skilled operator.

➤ Q bridge

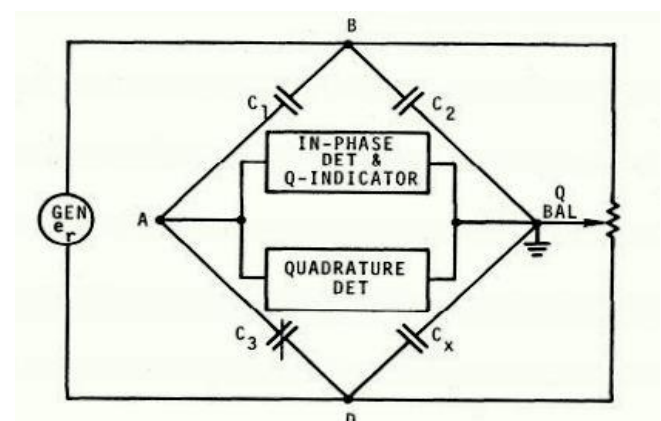


Fig. 2.9. Q bridge [1]

Fig. 2.9. presents the Q-bridge and the bridge equations [1] are as follows

$$C_x = \frac{C_1}{C_2} * \Delta C_3 \quad (2.14)$$

$$Q = \frac{e_0}{e_r} \quad (2.15)$$

The Q-bridge actually works on two principles, a situation made possible through the use of a phase sensitive detector. The unknown and known components are arranged in the Wheatstone's configuration, and the detector separated the unbalanced voltage between the points A and C into the in-phase and quadrature elements. The in-phase elements are due to the reactance unbalance. The balancing between the reactance is achieved by adjusting the in-phase unbalance voltage e_0 to the generator reference voltage e_r .

Advantages

- Has very range of measuring
- Versatile- can be used to for a wide variety of components

Disadvantages

- Low accuracy
- Slow
- Measuring range of Q is from 5 to 500

➤ Thurston bridge

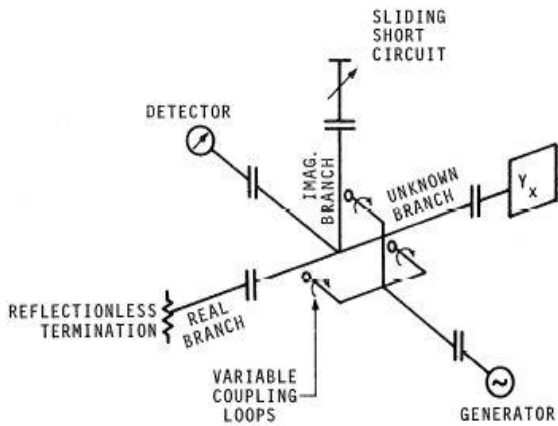


Fig. 2.10. Thurston bridge [1].

The Thurston bridge is presented in Fig. 2.10 and is a type of microwave bridge, it can be used for wide range of frequencies. The voltages are induced into the junction of the bridge branches, by means of conductive loops that are inductive in nature and the voltage induced is proportional to the angle of orientation of the plane of loops, with the center of conductors in the respect branch [1].

$$I = kVY \quad (2.16)$$

In equation (2.16), V is the generator voltage Fig. 2.10, Y is the branch admittance and k is the coupling coefficient, which is proportional to the angle of orientation of plane of the loop with center of the conductors.

Advantages

- Suitable only for measurements above 40MHz.
- Can be used to measure transistor parameters.
- Commercially available.

Disadvantages

- Low accuracy and resolution.
- Very slow.
- Cannot be used for measurements at low frequency.

➤ Young bridge

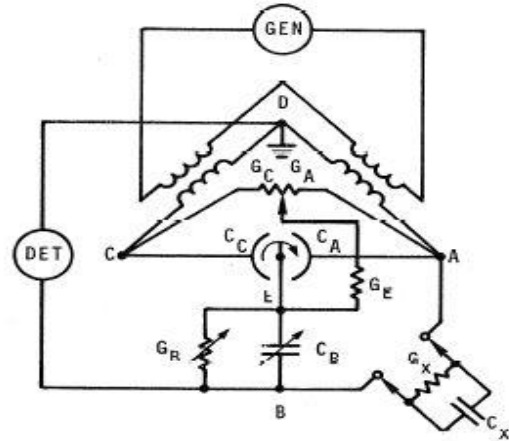


Fig. 2.11. Young bridge [1]

Fig. 2.11. presents the Young bridge and the balance condition equations [1] are

$$G_x = k(G_A - G_C) \quad (2.17)$$

$$C_x = k(C_A - C_C) \quad (2.18)$$

Where in the equations (2.17) and (2.18) G_x, C_x are the unknown conductance and capacitance.

This device is specially designed to measure small values of the capacitance. The working is based on the conversion principle of wye configuration [1] of admittance between the corners of the bridge A, B, in Fig. 2.11., and the capacitance is equivalent to the differential capacitor and conductance standards to maintain the constant and equal admittance in arms AB and BC Fig. 2.11.

Advantages

- Very useful for measuring very small admittances.
- Good accuracy.

Disadvantages

- Can be used for used only at fixed frequencies
- Higher frequency limit is 1 MHz
- Is slow.

2.2. Resonance method

Resonance methods are used when the Q value that is the ratio of reactance to the resistance is very high and are either connected series or parallel. Depending upon the arrangement either an ammeter or a voltmeter will be used as a detector. In both case unknown component value is determined by changing the frequency, or resistance or the reactance. In most case the variation of frequency is not a good option for high accuracy measurements because the frequency response versus the voltage (or current) is not symmetrical about the

resonant frequency so it can lead to errors. This method is ideal for three terminal measurements and cannot be used at frequencies that are closer to self-resonant frequency of any individual component. In series resonance measurement, the frequency and voltage are held constant. The circuit diagram is shown below

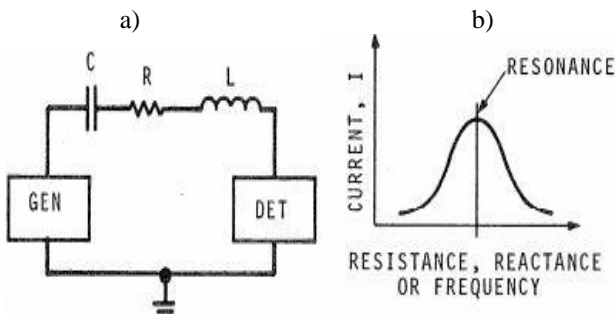


Fig. 2.12. Series resonance [1]

a) Circuit. b) Frequency response

The series resonance circuit and frequency response is shown in Fig. 2.12.

In all cases $\omega L = \frac{1}{\omega C}$, and for resistor variation we have the following result [1],

$$R_s = \frac{1}{\frac{I_{r1}}{I_{r2}} - 1} * R \quad (2.19)$$

The standard resistance, R, is removed and added in the circuit to lower the values of the resistance, R_s of the series circuit.

For reactance variations,

$$R_s = \frac{\omega(L - L_r)}{\sqrt{\left(\frac{I_r}{I}\right)^2 - 1}} \quad (2.20)$$

For frequency variations,

$$R_s = \frac{L(\omega - \omega_r)}{\sqrt{\left(\frac{I_r}{I}\right)^2 - 1}} \quad (2.21)$$

In parallel resonance measurements, variations in conductance, susceptance or frequency variation is used.

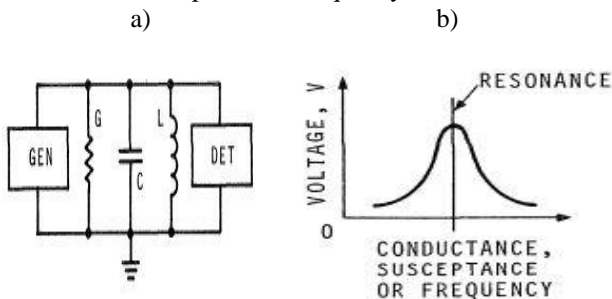


Fig. 2.13. Parallel resonance [1]

a) Circuit. b) Frequency response

Fig. 2.13.a) presents the parallel resonating circuit and b) represents the frequency response of the circuit. In all cases, $\omega L = \frac{1}{\omega C}$. In this method, the frequency and current are kept constant during the measurement. Voltages V_{r1} and V_{r2} are

observed as a means of standard conductance G, in and out of the circuit.

For conductance variation

$$G_p = \frac{1}{\frac{V_{r1}}{V_{r2}} - 1} * G \quad (2.22)$$

For variation in susceptance

$$G_p = \frac{\omega(C - C_r)}{\sqrt{\left(\frac{V_r}{V}\right)^2 - 1}} \quad (2.23)$$

For frequency variations,

$$G_p = \frac{C(\omega - \omega_r)}{\sqrt{\left(\frac{V_r}{V}\right)^2 - 1}} \quad (2.24)$$

The different kinds of resonance instruments are described below

➤ Q- Meter

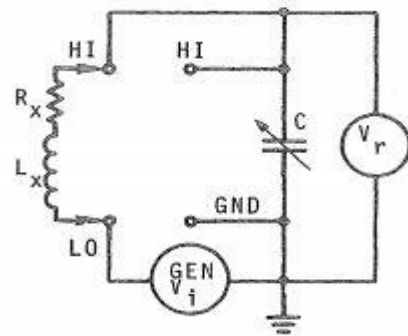


Fig. 2.14 Q-meter [1]

The Q-meter is presented in the Fig. 2.14 and is the widely used impedance measurement unit among the other available apparatus. It is available in many forms, the most common version reads directly in Q and the value of resonating capacitance, at particular frequencies in a direct visible scale of measurement. Q-meters which are equipped with a resistance used for the insertion of the test signal voltage cannot be used for making measurements across the components with external dc bias applied because of the risk of damage, due to external resistor or the thermo couple unit, or even the bias can affect the calibration of Q.

Measurement equations [1]

$$Q_x = \frac{\omega L_x}{R_x} = \frac{V_r}{V_1} \quad (2.25)$$

$$L_x = \frac{1}{\omega^2 * C_r} \quad (2.26)$$

Advantages

Analysis of Impedance Measurement Implementation Using Particular Sampling (By Lab View and Matlab)

- Easy to carry out measurements at different frequencies.
- Fast operation as compared to manual bridges.
- Wide frequency range.

Disadvantages

- Frequency monitoring is needed for accuracy.
- Uncertainty in Q due to high frequencies.

➤ Immittance trans-comparator

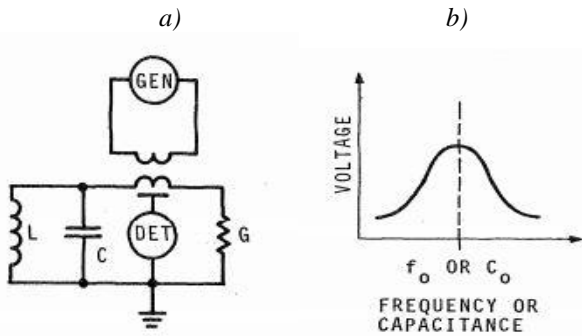


Fig. 2.15. Immittance trans-comparator [1]
a) Circuit diagram b) Frequency response

Fig. 2.15.a) presents an immittance trans-comparator circuit and b) represents the frequency response of the circuit. This equipment works on the principle of parallel resonance or anti-resonance. This can be used even for the measurement of di-electric constant. The machine build in various forms can be used either by changing the frequency or capacitance to measure the Q or the bandwidth of the parallel resonant circuit.

Measurement equations [1] are

$$Q = \frac{C_0}{\Delta C} = \frac{f_0}{\Delta f} \quad (2.27)$$

$$\omega L = \frac{1}{\omega C} \quad (2.28)$$

This is not a field instrument as it requires a highly stable and tunable source with more power capability.

Advantages

- Accuracy.
- Can be used for a wide range of frequencies and even can be used to measure positive and negative impedance.

Disadvantages

- Very slow operation.
- Need skilled operator.
- Capable only for measuring high Q value.

2.3. Active method

The actual definition of impedance is by Ohm's law, is the ratio of the complex voltage to the complex current

$$\vec{Z} = \frac{\vec{V}}{\vec{I}} \quad (2.29)$$

From the definition, active methods of measurement are defined as the measure of the ratio of complex voltage to complex current following the above condition stated by Ohm's law.

$$\vec{Z} = |Z| \angle \phi = \frac{|V| \angle \phi_v}{|I| \angle \phi_i} = \frac{|V|}{|I|} \angle \phi_v - \phi_i \quad (2.30)$$

Where $|Z|$, $|V|$, $|I|$ are the absolute magnitude values of the impedance, voltage and the current and the phase angles are represented by ϕ_z , ϕ_v , ϕ_i respectively. The different kinds of active instruments are:

➤ Vector impedance meter

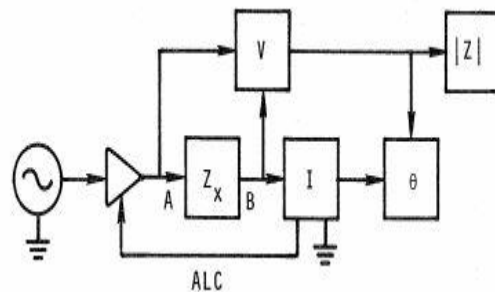


Fig. 2.16. Vector impedance meter [1]

The vector impedance meter is shown in Fig. 2.16. Measurement equations is as follows

$$\vec{Z} = \frac{E}{I} \quad (2.31)$$

These are the most recent devices and are convenient over the conventional bridges. Co-axial probes are used to connect the unknown component whose impedance is to be measured to the measuring circuit, and impedance magnitude and the phase angle can be read on the digital meter. The major applications are in testing, laboratories and also for design purposes.

Advantages

- Faster than bridges.
- No prior skills needed to operate.
- Versatile in nature, can be used for a wide range of frequencies.
- Wide range of measurements.

Disadvantages

- Low accuracy.
- Possibility of error at very high frequencies.

➤ L-C meter

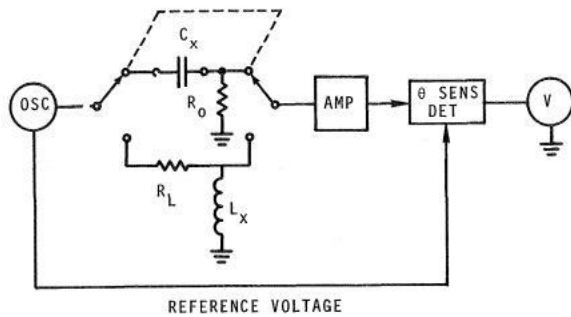


Fig. 2.17. L-C meter [1]

An LC-meter is presented in Fig. 2.17. Measurement equations [1] are as follows.

$$\frac{V_o}{V_i} \approx L \quad (2.32)$$

$$\frac{V_o}{V_i} \approx C \quad (2.33)$$

The L-C meter can only be used for measurement at fixed frequencies and does not provide any information about the resistance or conductance of tested reactance. The L-C meter sometimes is equipped to a dc output which is proportional to the inductance and capacitance that is measured and can be used to plot an XY graph using a plotter.

Advantages

- Faster measurement
- No operator experience needed
- Good accuracy
- Portability
- Linear dc output for data processing
- Easy to calibrate and is inexpensive.

Disadvantages

- Operates only in fixed frequencies
- Limited capacitance and inductance measurement.

III. IMPEDANCE ORTHOGONAL PART DETERMINATION METHODS

In this section, the different theoretical concepts and algorithms for impedance measurements are explained. The different DSP concepts like phase-sensitive detection, DFT, FFT, sine-fit algorithm, ellipse-fit algorithm, Goertzel filter and particular sampling are explained

3.1. Phase-sensitive detection

Phase-sensitive detection as shown in Fig. 3.1. and Fig. 3.2. is used to acquire very small signals in the presence of large additive noise. This concept led to the development of lock-in amplifiers, which makes this technique possible to execute. Lock-in amplifiers use the fact about time dependencies of a signal to extract it from a noise accumulated signal. A lock-in amplifier performs a signal multiplication to the input with a reference signal, this process is also called heterodyne detection, and then applies a low-pass filter to the result as shown in Fig. 3.3. This is called demodulation or phase-sensitive detection and recovers the signal the particular frequency that is in area of interest [3].

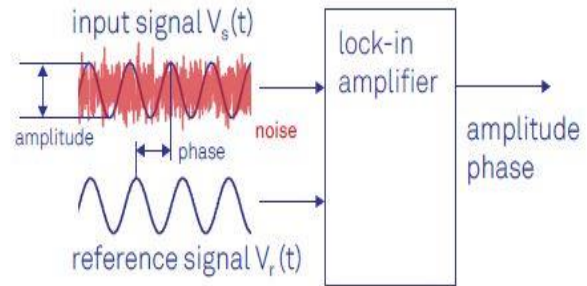


Fig. 3.1. Lock-in amplifier [2]

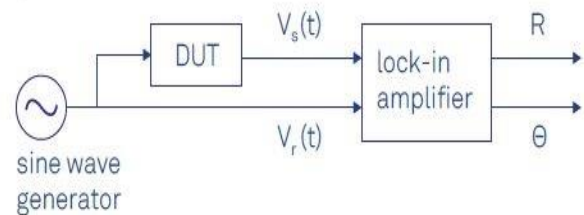


Fig. 3.2. Concept of lock-in amplifier [2]

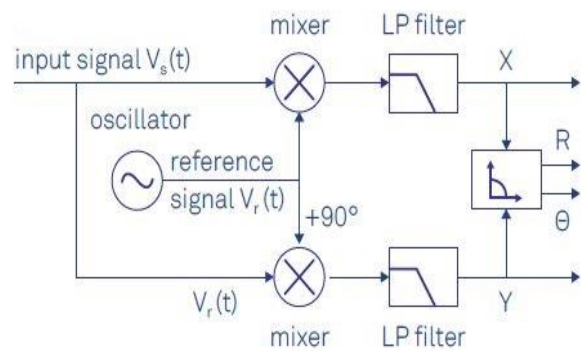


Fig. 3.3. Phase sensitive detection [2]

The reference signal is either generated by the lock-in amplifier or provided externally from a signal generator. The phase sensitive detection can be generally described as 6 stage process and they are described as follows [17].

- Modulation – The input signal is modulated or mixed up to a certain frequency
- Pre-amplification – A high-speed amplifier is used to amplify the signal to a desired level to feed to the circuit. Sometimes the amplification is also proceeded by a high pass filter in-order to remove the DC components in the signal.
- Reference signal – In most cases a pulse signal at the modulating frequency is used, it can be from a function generator or astable multi-vibrator.
- Multiplier – In this stage the pre-amplified signal is multiplied with the reference signal. The more generally used multiplier is an analog switch. The reference signal is used to open the analog switch periodically and letting the modulated input signal to pass through it.
- Integrator – The multiplied signal is passed through an integrator. Since the multiplied signals have a lot of frequency components in it, all of them will change to zero after integration, but the component that have the same phase and frequency remains non zero, and this component corresponds to the product of modulated signal with reference signal.

• Low pass filter – After the integration stage, the signal is demodulated to DC output. Due to presence of high frequency components we use low pass filter to filter the signal at certain frequency range.

Suppose f_1 and f_2 be two signal characterized by the following wave equation $f_1 = A \sin \omega_1 t$ and $f_2 = B \sin \omega_2 t$.

Now $f_1 * f_2$ is given by

$$AB \sin \omega_1 t \sin(\omega_2 t + \varphi) = -\frac{AB}{2} * \{ \cos[(\omega_1 + \omega_2) * t + \varphi] - \cos[(\omega_1 - \omega_2) * t - \varphi] \} \quad (3.1)$$

Let's integrate the product over the time $[0, T]$

$$\frac{1}{T} \int_0^T f_1 * f_2 dt = \frac{1}{T} \int_0^T -\frac{AB}{2} * \{ \cos[(\omega_1 + \omega_2) * t + \varphi] - \cos[(\omega_1 - \omega_2) * t - \varphi] \} dt \quad (3.2)$$

$$= -\frac{AB}{2T} \int_0^T \cos[(\omega_1 + \omega_2) * t + \varphi] dt + \frac{AB}{2T} \int_0^T \cos[(\omega_1 - \omega_2) * t - \varphi] dt \quad (3.3)$$

When $T \rightarrow \infty$, both the integral parts will be zero, except when $\omega_1 = \omega_2$ and $\varphi = 0$ the integration result is given by $\frac{AB}{2}$.

3.2. Discrete Fourier transform and Fast Fourier transform

DFT is the mathematical process of extracting the frequency components from a time domain signal. The DFT operates by comparing or correlating the signal to be analyzed against sinusoidal waveform or sinusoidal basis functions. The comparison is achieved by the mathematical operation called correlation as depicted in Fig. 3.4.

Correlation is either a measure of similarity of the signals or how strong the signal is present in the other. The analysis base signals used should be of the same length of the signal under processing. The sinusoidal basis functions are both sine waveforms and cosine waveforms. The comparison of the signal being analyzed with the sinusoidal basis functions results in complex numbers. The result of correlation of the signal with the sine wave sinusoidal basis function is stored as the imaginary value and the result of correlation of the signal being analyzed with the cosine wave sinusoidal basis function is stored as the real part as shown in Fig. 3.5.

The magnitude of the results of correlation is used to compute the magnitude spectrum. And from the complex number result the phase values are computed to obtain the phase spectrum.

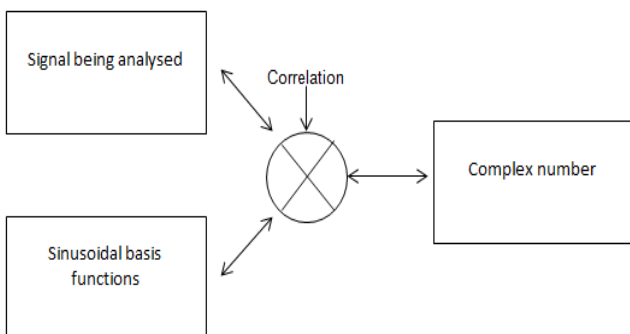


Fig. 3.4. Schematic showing working of DFT

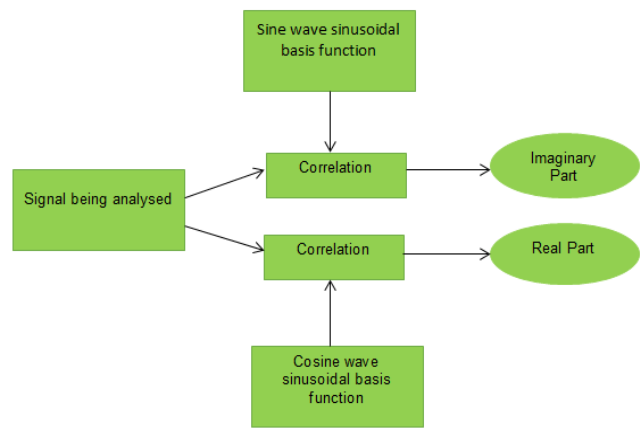


Fig. 3.5. Computation of real and imaginary part using correlation

The mathematical equation to compute DFT of a signal is described below,

For a discrete time signal $f(n)$, the N point DFT is defined as

$$F[k] = \sum_{n=0}^{N-1} f(n) e^{-\frac{j2\pi nk}{N}}, k = 0.1.2 \dots \dots \dots N - 1 \quad (3.4)$$

The matrix method to determine the DFT of the discrete time signal is given below

$$F_N = W_N f_n \quad (3.5)$$

$$\begin{pmatrix} F[0] \\ F[1] \\ F[2] \\ \vdots \\ F[N-1] \end{pmatrix} = \begin{pmatrix} 1 & 1 & 1 & 1 & \dots & 1 \\ 1 & W & W^2 & W^3 & \dots & W^{N-1} \\ 1 & W^2 & W^4 & W^6 & \dots & W^{N-2} \\ 1 & W^3 & W^6 & W^9 & \dots & W^{N-3} \\ \vdots & \vdots & \vdots & \vdots & \ddots & \vdots \\ 1 & W^{N-1} & W^{N-2} & W^{N-3} & \dots & W \end{pmatrix} \begin{pmatrix} f[0] \\ f[1] \\ f[2] \\ \vdots \\ f[N-1] \end{pmatrix} \quad (3.6)$$

In the equation (3.6), $f[0], f[1], f[2], \dots, f[N-1]$ represents the discrete time signal and $F[0], F[1], \dots, F[N-1]$ represents the corresponding DFT's and in the matrix W is called the twiddle factor matrix or matrix of linear transformation and given by

$$W = e^{-\frac{j2\pi}{N}} \text{ and } W = W^{2N} \quad (3.7)$$

The FFT is a fast algorithm used for computing the DFT. In FFT algorithm we divide calculations to compute 2-point, 4-point DFT's and generalize to 8-point, 16-point,....., 2^r point.

To compute the DFT of an N -point sequence using DFT equation (3.4) would take N^2 multiplications and additions. The FFT algorithm computes the DFT using $N \log_2 N$ multiplies and adds.

When we consider the cost of computation FFT is faster than DFT for big values of N To compute the DFT of an N -point sequence using the equation (3.4), would require N^2 complex multiplies and adds, which is together $4N^2$ complex multiplications and additions. There are $\frac{N}{2}$ butterflies per stage, and $\log_2 N$ stages, so that means about

$4 * \frac{N}{2} * \log_2 N = 2N \log_2 N$ real multiplies and $3N \log_2 N$ real adds for an N-point FFT.

Table 3.1. Cost of calculation comparison of DFT and FFT

N	Total DFT calculations $4N^2$	Total FFT calculations $2N \log_2 N$	Speedup
2	16	4	4
4	64	16	4
8	256	48	5
1024	419304	20480	205
65536	$1.7 * 10^{10}$	$2.1 * 10^6$	10^4

3.3. Sine-fit algorithm

Sine-fit algorithms are an option to estimate the sine-signal parameters from a set of acquired samples. Sine-fit algorithms were standardized for the characterization of ADCs [11] [12]. There are three parameter-sine fitting, four parameter-sine fit and seven parameter-sine fit algorithms. The main objective is to find a set of parameters to the fitting model (analytical expression of a sine signal) that minimizes the sum of the squared errors between the model and the sampled data. In three parameter sine fit version, the phase, amplitude and DC components of an acquired sine wave when the signal rate is known and is a multiple linear regression method that requires no iterations. In the four parameters algorithm, the rate frequency is also calculated which makes the model and requires an iterative non-linear least squares procedure in order to obtain the best parameters. The convergence of the algorithm depends on the initial calculations of the parameters. For two channel systems with a common signal frequency, as is the case of impedance measurements, all the information from both records should be used to obtain a better calculate of the common rate of occurrence. This is obtained with the seven parameter sine fit which is also an iterative algorithm much like four parameter. The main difference is that it calculates, in each iteration, the two amplitudes, the two phases, the two DC items and the common frequency. The effectiveness of this method will be demonstrated by smaller Cramer Rao lower Bound (CRLB) of the frequency and phase difference when compared with the application of two four parameters sine-fit. In the seven parameter sine-fit [12], the calculated parameter vector for each iteration is

$$\mathbf{x}^{(i)} = [A_1^{(i)} \ B_1^{(i)} \ C_1^{(i)} \ \Delta f^{(i)} \ A_2^{(i)} \ B_2^{(i)} \ C_2^{(i)}]^T \quad (3.8)$$

Where A_k and B_k in equation (3.8), are the in-phase and quadrature amplitudes from which the sine amplitudes D_k and phases ϕ_k are obtained. Δf^i is the correction that updates the calculated common frequency. The iteration process ends when the relative rate of occurrence adjustment $\frac{\Delta f^i}{f}$ is below a present threshold. After the Iterative part of the algorithm is completed and the frequency is determined, the amplitudes A_k and B_k are determined with the three parameter sine fit. The calculated parameter vector is obtained from

$$\mathbf{x}^{(i)} = [[\mathbf{D}^{(i)}]^T \mathbf{D}^{(i)}]^{-1} [[\mathbf{D}^{(i)}]^T \mathbf{y}] \quad (3.9)$$

Where y is the concatenated sample vector

$$\mathbf{y} = [u_{1,1} \ u_{1,2} \ \dots \ u_{1,N} \ u_{2,1} \ u_{2,2} \ \dots \ u_{2,N}]^T \quad (3.10)$$

And

$$\mathbf{D}^{(i)} = \left[\begin{array}{c|c|c} \mathbf{Q}_1^{(i)} & \mathbf{r}_1^{(i)} & \mathbf{0} \\ \hline \mathbf{0} & \mathbf{r}_2^{(i)} & \mathbf{Q}_2^{(i)} \end{array} \right] \quad (3.11)$$

With ($\omega=2\pi f^i$)

$$\mathbf{Q}_k^{(i)} = \begin{bmatrix} \cos(\omega t_{k,1}) & \sin(\omega t_{k,1}) & 1 \\ \cos(\omega t_{k,2}) & \sin(\omega t_{k,2}) & 1 \\ \vdots & \vdots & \vdots \\ \cos(\omega t_{k,N}) & \sin(\omega t_{k,N}) & 1 \end{bmatrix} \quad (3.12)$$

And

$$\mathbf{r}_k^{(i)} = \begin{bmatrix} \alpha_{k,1} \\ \alpha_{k,2} \\ \vdots \\ \alpha_{k,N} \end{bmatrix} \text{ with } \alpha_{k,n} = -2\pi A_k^{(i)} t_{k,n} \sin(\omega t_{k,n}) + 2\pi B_k^{(i)} t_{k,n} \cos(\omega t_{k,n}). \quad (3.13)$$

The calculation of \mathbf{D}^i requires $2N*7$ words (in DSP execution, each word usually corresponds to a 32-bit long single accurate float $[\mathbf{D}^{(i)}]^T \mathbf{D}^i$ requires an additional $7*7$ words while $[\mathbf{D}^{(i)}]^T \mathbf{Y}$ requires 7 words. Overall, the technique requires $17N + 63$ words [11] (the $17N$ part corresponds to $2N$ for the samples, $14N$ for \mathbf{D}^i and $1N$ for FFT used in the interpolated discrete Fourier transform to calculate the initial frequency. Due to the restricted DSP internal memory and the space occupied by the program itself and other internal variables, the number of samples N is limited.

$$[\mathbf{D}^{(i)}]^T \mathbf{D}^{(i)} = \begin{bmatrix} E_{1,1} & E_{1,2} & E_{1,3} & E_{1,4} & 0 & 0 & 0 \\ E_{1,2} & E_{2,2} & E_{2,3} & E_{2,4} & 0 & 0 & 0 \\ E_{1,3} & E_{2,3} & N & E_{3,4} & 0 & 0 & 0 \\ E_{1,4} & E_{2,4} & E_{3,4} & E_{4,4} & E_{4,5} & E_{4,6} & E_{4,7} \\ 0 & 0 & 0 & E_{4,5} & E_{1,1} & E_{1,2} & E_{1,3} \\ 0 & 0 & 0 & E_{4,6} & E_{1,2} & E_{2,2} & E_{2,3} \\ 0 & 0 & 0 & E_{4,7} & E_{1,3} & E_{2,3} & N \end{bmatrix} \quad (3.14)$$

With

$$E_{1,1} = \sum_{n=1}^N \cos^2(\omega t_n), E_{1,2} = \sum_{n=1}^N \cos(\omega t_n) \sin(\omega t_n), \quad (3.15)$$

$$E_{1,3} = \sum_{n=1}^N \cos(\omega t_n), E_{1,4} = \sum_{n=1}^N \cos(\omega t_n) \alpha_{1,n}, \quad (3.16)$$

$$E_{2,2} = \sum_{n=1}^N \sin^2(\omega t_n), E_{2,3} = \sum_{n=1}^N \sin(\omega t_n), E_{2,4} = \sum_{n=1}^N \sin(\omega t_n) \alpha_{2,n} \quad (3.17)$$

$$E_{3,4} = \sum_{n=1}^N \alpha_{1,n}, E_{4,4} = \sum_{n=1}^N (\alpha_{1,n}^2 + \alpha_{2,n}^2), \quad (3.18)$$

$$E_{4,5} = \sum_{n=1}^N \cos(\omega t_n) \alpha_{2,n}, E_{4,6} = \sum_{n=1}^N \sin(\omega t_n) \alpha_{2,n}, E_{4,7} = \sum_{n=1}^N \alpha_{2,n}. \quad (3.19)$$

$[\mathbf{D}^{(i)}]^T \mathbf{D}^{(i)}$ is a symmetric matrix. Finally for $[\mathbf{D}^{(i)}]^T \mathbf{Y}$

$$[\mathbf{D}^{(i)}]^T \mathbf{y} = \begin{bmatrix} \sum_{n=1}^N \cos(\omega t_n) u_{1,n} \\ \sum_{n=1}^N \sin(\omega t_n) u_{1,n} \\ \sum_{n=1}^N u_{1,n} \\ \sum_{n=1}^N u_{1,n} \alpha_{1,n} + u_{2,n} \alpha_{2,n} \\ \sum_{n=1}^N \cos(\omega t_n) u_{2,n} \\ \sum_{n=1}^N \sin(\omega t_n) u_{2,n} \\ \sum_{n=1}^N u_{2,n} \end{bmatrix}. \quad (3.20)$$

With this method the memory usage is reduced to $3N + 63$ (the $3N$ part corresponds to $2N$ for the samples and $1N$ for the FFT used). For the initial \mathbf{A}_k and \mathbf{B}_k calculates, the three-parameter sine-fit is applied to each channel using the rate of occurrence obtained with the IpDFT. These two algorithms are also executed in the DSP. Samples acquired with the proposed system at 1 kHz measurement frequency is sampled at 48 kS/s are shown together with the reconstructed sine signals using the seven parameter algorithm are shown in Fig. 3.6.

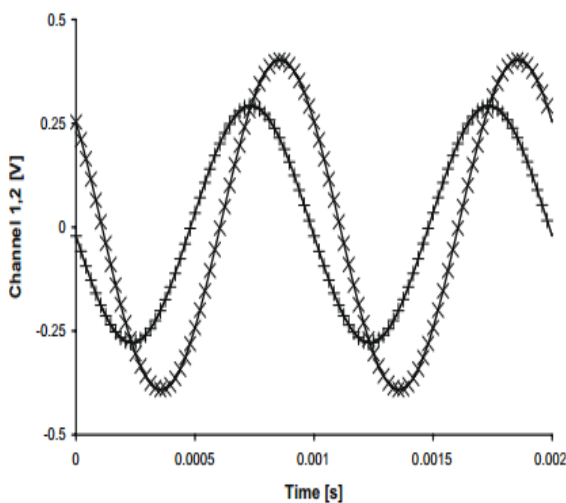


Fig. 3.6. Acquired samples from two channels with (+) for channel 1 and (x) for channel 2 and the corresponding sine-fit reconstructed signals (lines). [16]

3.4. Ellipse-fit algorithm

The ellipse-fit algorithm estimates the ellipse parameters that best fit the XY pairs of voltages from the two channels. From the ellipse parameters, the sine amplitudes, dc items and the phase difference are determined [11] [12]. The ellipse-fit algorithm is a non-iterative method based on Lagrange multipliers. The refined execution, first published requires the construction of small matrices (3×3) instead of the $N \times 3$ large matrix used in their multiplication and inversion and also determination of the eigenvectors of a 3 by 3 matrix. Through mathematical manipulation the common frequency can be removed

$$\left(\frac{u_1 - C_1}{D_1}\right)^2 + \left(\frac{u_2 - C_2}{D_2}\right)^2 - 2 \frac{(u_1 - C_1)(u_2 - C_2)}{D_1 D_2} \times \cos(\Delta\phi) - \sin^2(\Delta\phi) = 0. \quad (3.21)$$

equation (3.21). corresponds to a conic

$$F(u_1, u_2) = au_1^2 + bu_1u_2 + cu_2^2 + du_1 + eu_2 + g = 0, \quad (3.22)$$

Which describes an ellipse when,

$$b^2 - 4ac < 0. \quad (3.23)$$

By introducing a scaling constraint q , this condition can be set to $4ac - b^2 = 1$. For conic to correspond to ellipse three conditions must be verified $D_1 - 0$; $D_2 - 0$ and $\cos^2(D_1) < 1$, either a line segment (whenever least one of conditions is not true) or an ellipse. From the ellipse parameters, the sine parameters are obtained through

$$D_1 = \frac{1}{\sqrt{qa}}, D_2 = \frac{1}{\sqrt{qc}}, \quad (3.24)$$

$$C_1 = \frac{2cd - be}{b^2 - 4ac}, C_2 = \frac{2ae - db}{b^2 - 4ac} \quad (3.25)$$

And

$$\cos(\Delta\phi) = -\frac{\text{sign}(q) \times b}{2\sqrt{ac}}. \quad (3.26)$$

$$\frac{D_2}{D_1} = \sqrt{\frac{a}{c}} \quad (3.27)$$

Therefore the scaling constant q does not need to be determined. Also, the sign of parameter a (due of the scaling constant, required can be replaced by the sign of parameters a & c can both be negative which corresponds also to $q < 0$). The only parameter that needs further calculation is the sign of D_1 which is unavailable but can be retrieved from the rotation direction of the ellipse, if the ellipse is constructed clockwise $D_1 > 0$ and $D_1 < 0$ if it is constructed counterclockwise. The sign of the phase difference between two consecutive sample pairs [11]

$$\delta_n|_{n=1, \dots, N-1} = \text{sign} \left\{ \arg \left[u_{1,n+1} - \frac{1}{N} \sum_{i=1}^N u_{1,i} + j \left(u_{2,n+1} - \frac{1}{N} \sum_{i=1}^N u_{2,i} \right) \right] \right. \\ \left. - \arg \left[u_{1,n} - \frac{1}{N} \sum_{i=1}^N u_{1,i} + j \left(u_{2,n} - \frac{1}{N} \sum_{i=1}^N u_{2,i} \right) \right] \right\} \quad (3.28)$$

can be used to determine whether the ellipse is being constructed clockwise or counterclockwise. The ellipse center is calculated using all the required samples. However, due to the presence of noise, some of the consecutive samples may give the wrong rotation direction, therefore voting system was executed. The sign of the sum of the defined also determines the sign of D_1 [11]

$$\text{sign}(\Delta\phi) = -\text{sign} \left(\sum_{n=1}^N \delta_n \right). \quad (3.29)$$

The ellipse-fit requires $2N + 42$ words [11] ($2N$ for the samples, four 3 by 3 matrix and two element vectors). With the current sine-fit exestuation, the memory needed by the ellipse-fit is not a big improvement from the memory needed by the seven-parameter sine-fit. The main merit is the total number of operation - not only for the matrix construction and manipulation but also due to the fact that sine-fit is iterative and the ellipse-fit is not, examples acquired at 48 kS/s with the purposed system at 1 kHz measurement frequency are shown together with the reconstructed ellipse obtained using the ellipse-fit. Is shown in Fig. 3.7

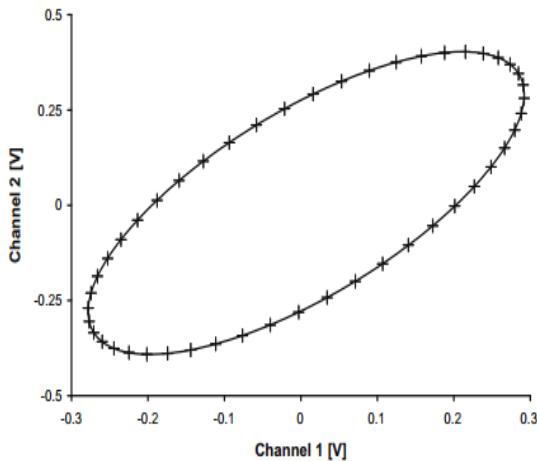


Fig. 3.7. Acquired samples from two channels (+) and the corresponding reconstructed ellipse (line).[16]

3.5. Goertzel's algorithm

Goertzel algorithm is used to minimize the computation cost of DFT by almost a factor of two. It is useful in applications that require only a few DFT frequency samples.

Some applications like frequency shift keying demodulation or DTMF, where typically two frequencies are used to transmit binary data, the circuit is designed only to identify the line for two simultaneous frequencies. Goertzel algorithm reduces the complex multiplication for computing the DFT relatively by a factor of two to the direct computation using the equation (3.30). Goertzel algorithm is derived by

converting the DFT equation (3.30), into a form of convolution which is an equivalent form for the DFT equation (3.30). For detailed description the Goertzel algorithm is explained by terms of mathematical equations

The DFT $X[k]$ of a disc $x(n)$ is given, (3.28)
(4.11)

$$X[k] = \sum_{n=0}^{N-1} x(n) e^{-j2\pi nk/N} \quad k = 0.1.2 \dots N-1 \quad (3.30)$$

$$= \sum_{n=0}^{N-1} x(n) W_N^{nk} \quad (3.31)$$

Where $W = e^{-j2\pi/N}$ and $W = W^{2N}$

$$= \sum_{n=0}^{N-1} x(n) W_N^{nk} \quad (3.29) \quad (4.11) \quad (3.32)$$

$$= \sum_{n=0}^{N-1} x(n) W_N^{(N-n)k} \quad (3.34)$$

$$= ((W_N^{-k} x(0) + x(1)W_N^{-k} + x(2)W_N^{-k} + \dots + x(N-1)W_N^{-k}) \quad (3.35)$$

The expression in the equation (3.35) can be expressed as a recursive equation,

$$y(n) = W_N^{-k} y(n-1) + x(n) \quad (3.36)$$

Where $y(-1) = 0$, The coefficients will be equal to the output of difference equation at time $n=N$.

$$X(k) = y(N) \quad (3.37)$$

Expressing the difference equation in terms of Z-transform and the resulting transfer function can be obtained by multiplying the numerator and denominator by $1 - W_N^k z^{-1}$,

$$\frac{Y(z)}{X(z)} = H(z) = \frac{1}{1 - W_N^k z^{-1}} = \frac{1 - W_N^k z^{-1}}{1 - ((W_N^k + W_N^k)z^{-1} - z^{-2})} = \frac{1 - W_N^k z^{-1}}{1 - (2 \cos \frac{2\pi k}{N}) z^{-1} - z^{-2}} \quad (3.38)$$

The realization of Goertzel system is represented below in Fig. 3.8

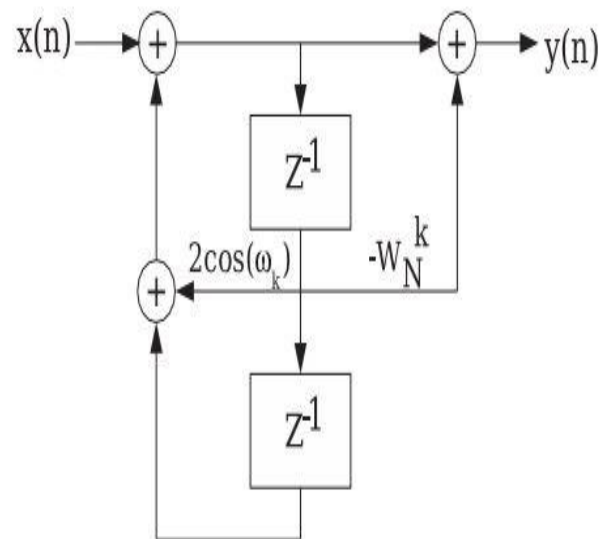


Fig. 3.8. Realization of Goertzel system

We do not compute $y(n)$ for all values of n , but only for $n = N$. It implies that we compute only the recursive part, or just the left side in the graphical representation of the realization Fig. 3.8. for $n = [0, 1, \dots, N]$, which involves only one real and complex product rather than a complex and complex product as in a direct DFT, plus one complex multiplication to get $y(N) = X(k)$.

IV. PARTICULAR SAMPLING METHOD IMPLEMENTATION.

The particular sampling method is based on taking signal samples in exactly determined time moments, allowing to simply calculating the vector of fundamental harmonic of the measurement signal. When comparing to DFT, the particular sampling method uses only a summation of the collected samples, and the obtained two sums determine the orthogonal parts of the calculated sinusoidal signal.

Table 4.1. Example values and eliminated harmonics[4]

q_i	Eliminated harmonics
3	3, 9, 15, 21, 27, 33, 39, 45, 51,...
5	5, 15, 25, 35, 45, 55, 65, 75,...
7	7, 21, 35, 49, 63, 77,...
11	11, 33, 55, 77, 99,...
13	13, 39, 65, 91,...
17	17, 51, 85,...
19	19, 57, 95,...
23	23, 69,...

To determine orthogonal parts of voltage and current proportional signals we need to acquire samples and calculate two sums for each signal. Each sum items have “+” or “-“ signs depending on parameter m . For easier implementation, we separate items of each sum for those with “+” sign (Re_p and Im_p) and those with “-“ sign (Re_m and Im_m). The main aim for this implementation of the particular sampling algorithm is determination of the orthogonal parts of the fundamental harmonic, but not removing the possibly high number of higher harmonics, so the Q was assumed as equal 2 and according to Table 4.1, $q_1 = 3$ and $q_2 = 5$. To correctly realize the particular sampling method (to sample at certain time moments) it is necessary to assure the sampling frequency f_s is related to measurement frequency f :

For assumed values of $Q=2$, $q_1=3$ and $q_2=5$ the formula can be evaluated as below: and this means that for the assumed parameters, the sampling frequency should be at least 60 times or higher than the measurement frequency, we need to acquire 60 samples during a measurement signal period. Using the defined V value, we can express sampling moments as a sample number by entering a variable D (given in degrees).

Table 4.2. Sampling schedule for the proposed particular sampling method implementation[4]

Sum iteration number	Sampling moment according to (11) and (12)		Sampling moments expressed as D multiple – sample number			
	Re component	Im component	Re_p	Re_m	Im_p	Im_m
1	$-x$	$-(x+90)$		1		15
2	$x+180$	$x+90+180$	30		45	
3	$-(x+\frac{180}{3})$	$-(x+90+\frac{180}{3})$		10		25
4	$x+180+\frac{180}{3}$	$x+90+180+\frac{180}{3}$	40		55	
5	$-(x+\frac{180}{5})$	$-(x+\frac{180}{5})$		6		21
6	$x+180+\frac{183}{5}$	$x+90+180+\frac{183}{5}$	36		51	
7	$-(x+\frac{180}{3}+\frac{180}{5})$	$-(x+90+\frac{180}{3}+\frac{180}{5})$		16		31
8	$x+180+\frac{180}{3}+\frac{180}{5}$	$x+90+180+\frac{180}{3}+\frac{180}{5}$	46		61=1	

The sample numbers given in Table 4.2 above can be directly used in software for calculation of Re_m and Im_m parts of voltage and current.

4.1. Particular sampling method implementation test by simulation

The particular sampling method presented will be first implemented as a Matlab script and tested. As a reference the DFT-based method was used assuming the same sampling frequency: all acquired samples containing one period of the measurement signal were used for DFT, but selected samples were used for the particular sampling method. To create a simulation situation similar to the real-life one, the generated sinusoidal signal has a white-noise signal (normal distribution) and 50 Hz noise added (reflecting Interference caused by power lines).

The Matlab program simulates the experimental setup and compares the impedance values that are calculated using the DFT algorithm and then simultaneously also using the concept of Particular sampling. The program is intended to calculate the theoretical phase difference error and the error in signal ratio which the relative error in calculating the impedance using particular sampling.

After the simulation the graphs resulting in the phase difference error and signal ratio error are obtained.

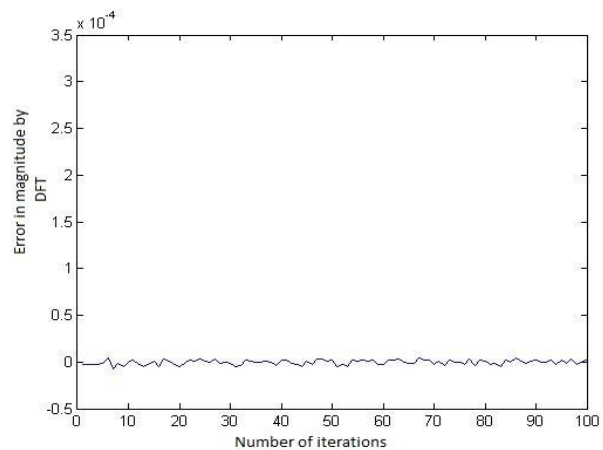


Fig. 4.1. Error in magnitude estimation by DFT using matlab simulation

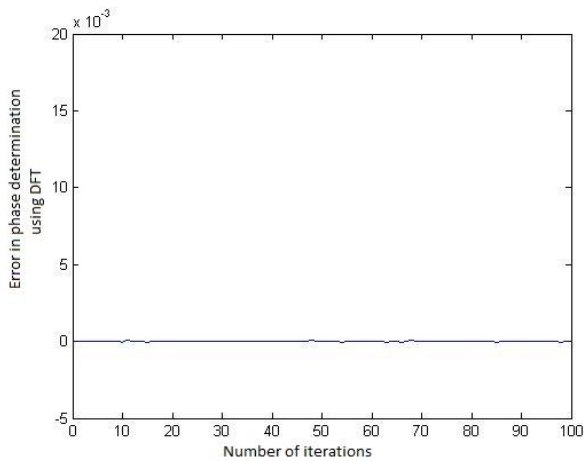


Fig. 4. 2. Error in phase determination using DFT by matlab simulation

Fig. 4.1. and Fig. 4.2. shows the error in determining the magnitude and phase respectively using DFT, as a means of matlab simulation for 100 iterations

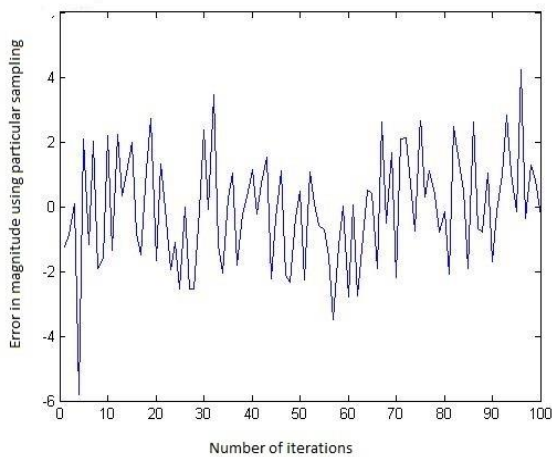


Fig. 4.3. Error in magnitude estimation by particular sampling using matlab simulation

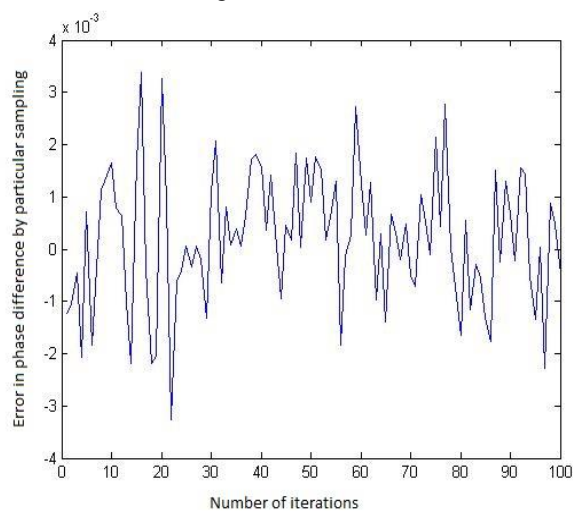


Fig. 4.4. Error in phase determination by particular sampling using matlab simulation

Fig. 4.3. and Fig. 4.4. shows the error in determining the magnitude and phase respectively using particular sampling, as a means of matlab simulation for 100 iterations.

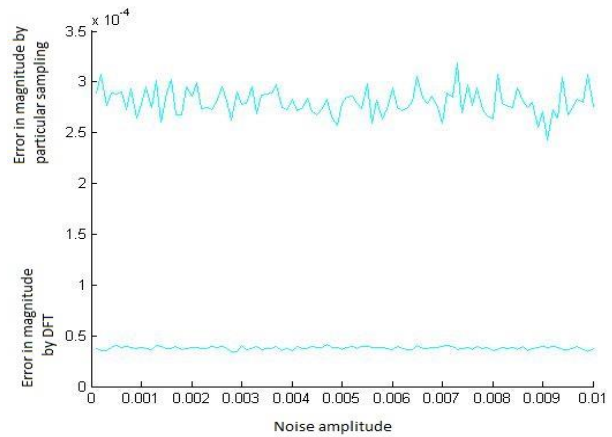


Fig. 4.5. Noise amplitude versus the error in magnitude by DFT and particular sampling using matlab simulation

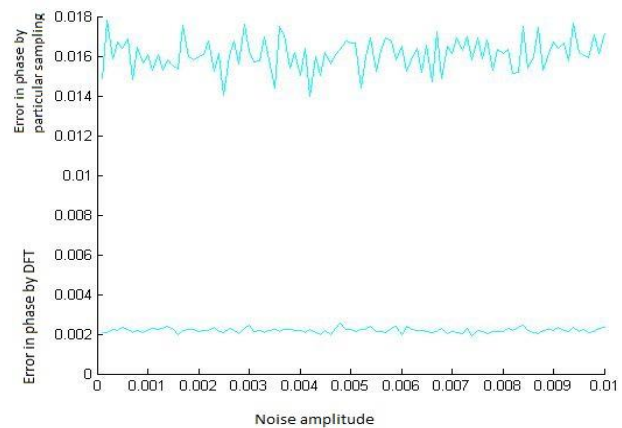


Fig. 4.6. Noise amplitude versus the error in phase difference by DFT and particular sampling using matlab simulation

Fig. 4.5. shows the error in determining the magnitude and phase respectively using DFT versus noise amplitude and Fig. 4.6. shows the error in determining the magnitude and phase respectively using particular sampling versus noise amplitude using matlab simulation.

As a result of simulation it can be noted from the Fig. 4.1. and Fig. 4.2. that the error in computing the impedance using particular sampling is more as compared to the computation using DFT. From Fig. 4.3. and Fig. 4.4., the error in determining the phase using particular sampling is more in magnitude as compared to error by using DFT. For low frequencies the particular sampling method is more prone to noise as it can be observed from Fig. 4.5. and Fig. 4.6. the error rate increase as frequency increase as due to the fact that there is some data loss when a part of samples are considered

4.2. Particular sampling-based impedance measurement method implementation in PSoC

A block diagram and a view of the measurement system prototype for experimental evaluation of the particular sampling method implementation are shown in Fig. 4.7.a) and Fig. 4.7.b). The system consists of 3 parts: a PC computer which allows to control the device and visualize [4].

Thanks to the use of PSoC, the number of items was reduced to the minimum. The used PSoC generation represents microcontrollers with relatively low processing power and small RAM memory. The prototype was built using a CY8C29566 chip with 2 kB SRAM memory. The

sinusoidal excitation signal applied to the calculated impedance is produced using the DDS method with the aid of a D/A converter DAC1, on the basis of sine samples placed in PSoC's RAM memory (GENbuf). TIMER1 creates a clock signal which controls generation and acquisition using the microcontroller clock. The DAC1 output signal before application to the impedance under test is first filtered in a low-pass filter removing unwanted stair-steps.

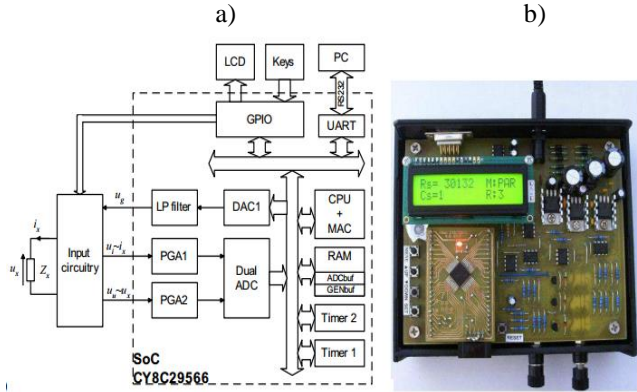


Fig. 4.7. Block diagram (a) and a view of prototype (b) of the particular sampling method PSoC implementation. [4]

4.3. Implementation in form of Labview application using DAQ card

In this method, a DAQ card is used to produce the excitation signal that is the voltage signal that is used to find the impedance. The FFT of the signal is taken and displayed as phase and amplitude spectrum. The excitation signal is passed through the circuit under test and the current through the circuit is observed and voltage across it is calculated. The resultant values are then transformed to FFT and its phase and amplitude spectrum is observed, thus the impedance can be observed by dividing the amplitudes and subtracting the phases. The particular sampling method is based on taking signal samples in precisely determined time moments, allowing to simply calculate the vector of fundamental harmonic of the measurement signal. When comparing to DFT, the particular sampling method uses only a summation of the collected samples, and the obtained two sums determine the orthogonal parts of the measured sinusoidal signal.

The front panel of the signal generator developed by the labview application is shown below in Fig. 4.8.

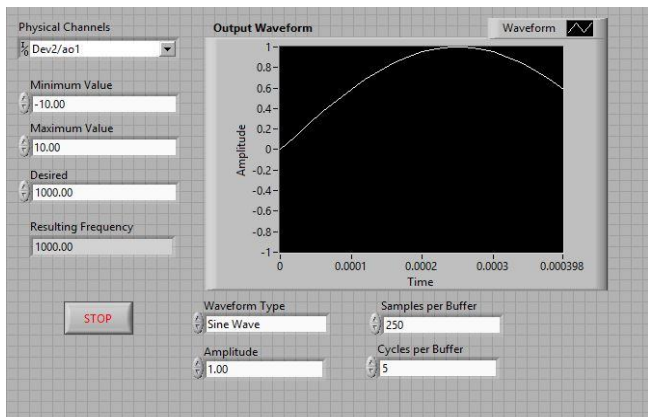


Fig. 4.8. Front Panel of labview application for signal generation

The application provides functionality to the user to generate the different kinds of waveform, change the amplitude and frequency of the signal. The Cycles per buffer is the number of cycles viewed on the display and most preferably it is set to 1.

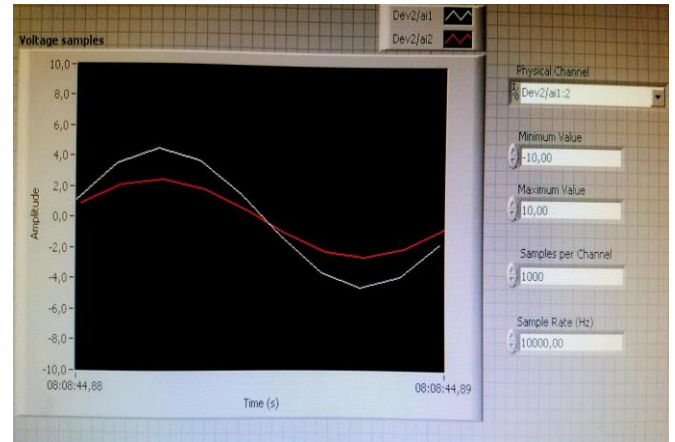


Fig. 4.9. Front panel of labview application for sample acquisition

The application provides the functionality to change the sampling frequency to obtain different sampling ratios which are useful for experiments and is shown in Fig. 4.9. There are two channels, whose signals are acquired using the DAQ as shown in Fig. 4.10. to analyze the error in the method devised



Fig. 4.10. DAQ card NI USB - 6251 used for experiment [19]

Experimental setup

An excitation signal is generated using the DAQ NI USB 6251, to the circuit as shown in Fig. 4.11.

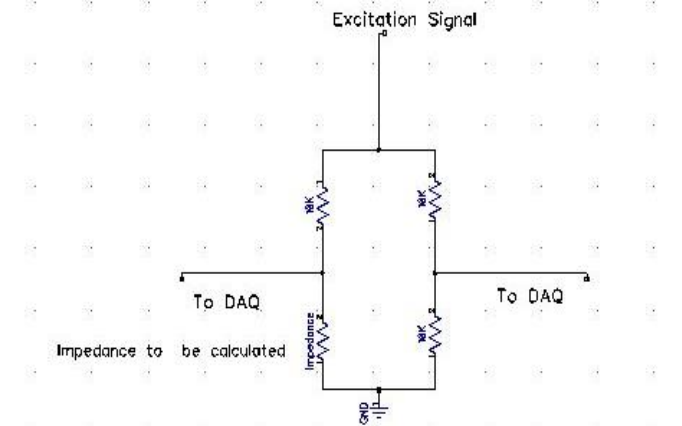


Fig. 4.11. Circuit diagram showing experimental setup (DIPTRACE software)

This is actually a bridge setup where the impedance to be found is connected to the unknown terminal and the known impedances are connected to other terminals. The excitation signal is sine wave and the signal are back fed to DAQ and processed by the lab view application to compare the phase difference and the ratio of the signal amplitude using FFT and particular sampling. Since the application provides the ability to the user to change amplitude, frequency, cycles per buffer. The experiment procedure is as follow

- Varying the amplitude of the signal for 3 different volts as 1 volt, 3volts and 5 volts.
- Varying the sampling ratio to 60, 80, 100- by changing the sampling frequency
- Adding additional component in the impedance to be calculated
- Incrementing the sample index that are used to obtain the particular samples
- Varying the frequency of the signal

Experiment 1- Using only resistor in all positions

Resistors of value 10K are connected in all terminals. The amplitude of the signal is varied from 1, 3 and 5 Volts and the frequency varied from 0.1, 1, 10, 100, 500, 1000, 2500, 5000 Hz and also the sampling ratio that is the ratio of sampling frequency to actual frequency is varied from 60 80 and 100. All of which has been carefully depicted in graphical representation.

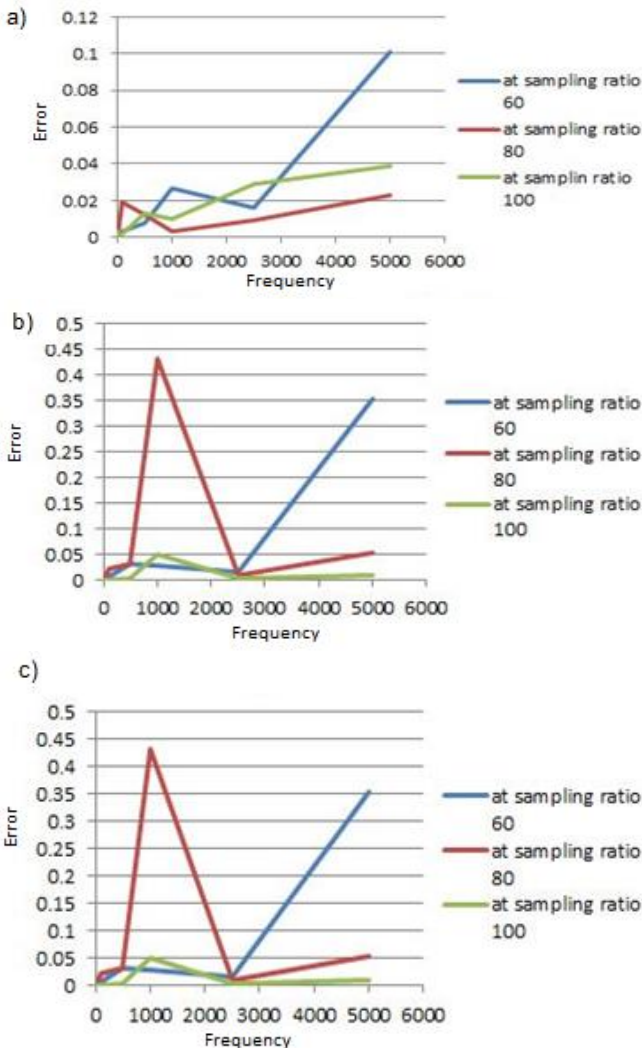


Fig. 4.12. Error in phase difference

a) Using 1 Volt, b) Using 3 Volts, c) Using 5 Volts

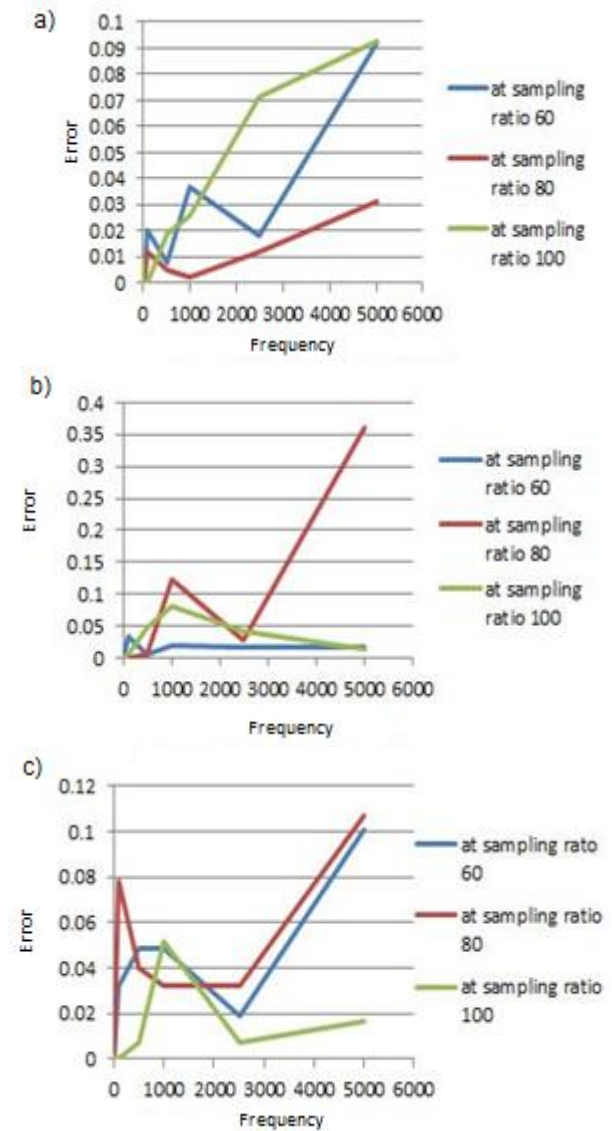
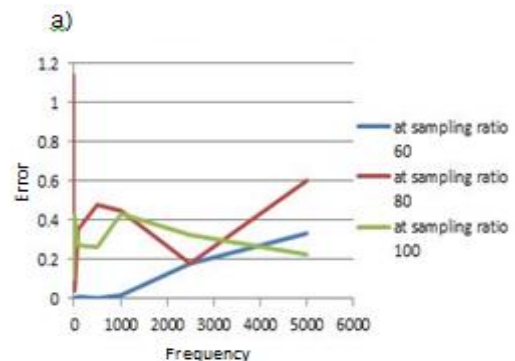


Fig. 4.13. Error in signal ratio

a) Using 1 Volt, b) Using 3 Volts, c) Using 5 Volts.

The experimental results for the error in phase difference and signal ratio for different voltages 1 V, 3 V and 5V, and different sampling ratios 60, 80 and 100 are shown in Fig. 4.12 and Fig. 4.13.

Experiment with an additional capacitor connected parallel to resistor The resistor of value 10K and a capacitor of 100 pF are connected parallel across the terminal for impedance measurement



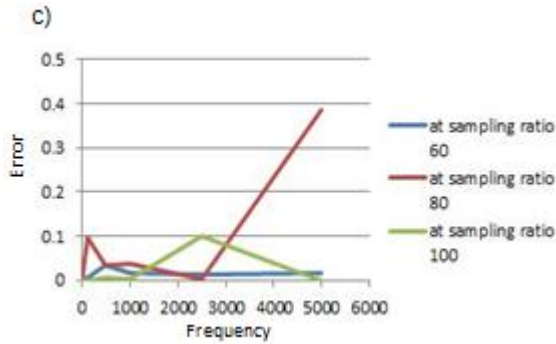
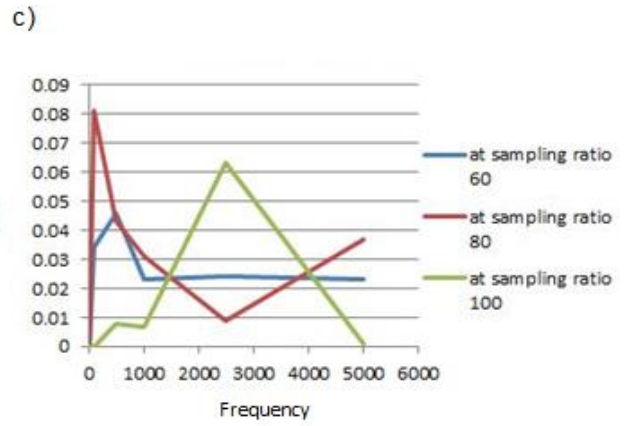
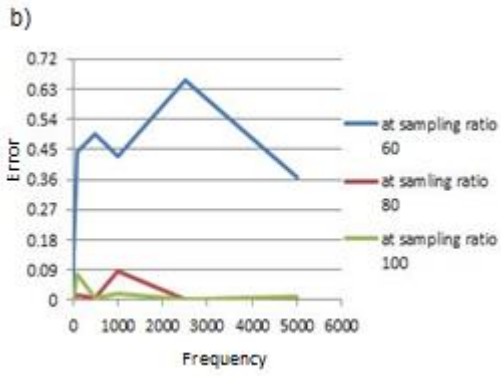


Fig. 4.14. Error in phase difference

a) Using 1 Volt, b) Using 3 Volts, c) Using 5 Volts

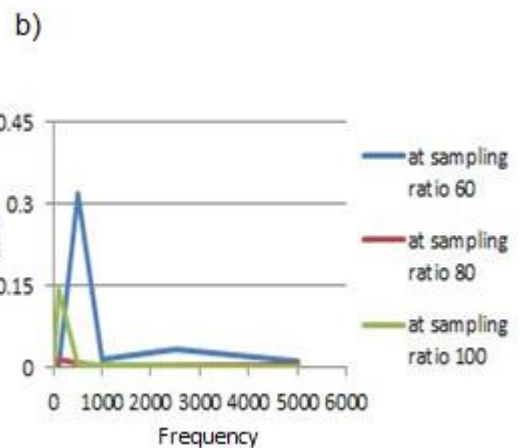
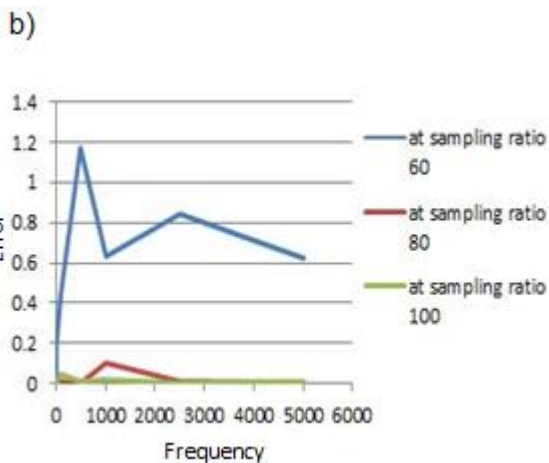
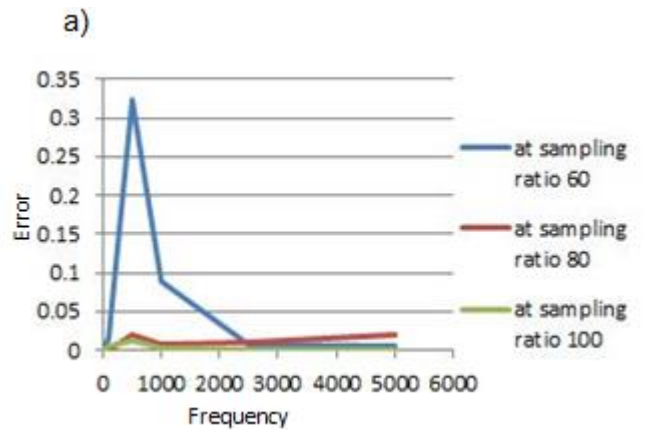
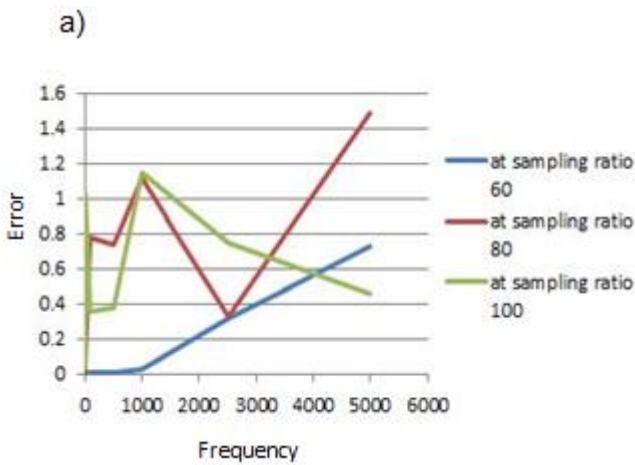


Fig. 4.15. Error in signal ratio

a) Using 1 Volt, b) Using 3 Volts, c) Using 5 Volts.

The experimental results for the error in phase difference and signal ratio for different voltages 1 V, 3 V and 5V, and different sampling ratios 60, 80 and 100 are shown in Fig. 4.14. and Fig. 4.15.

Experiment 3 - With additional two capacitors connected parallel to resistor.

The resistor of value 10K and two capacitors of values 100 pF and 100 nF are connected parallel across the terminal for impedance measurement.

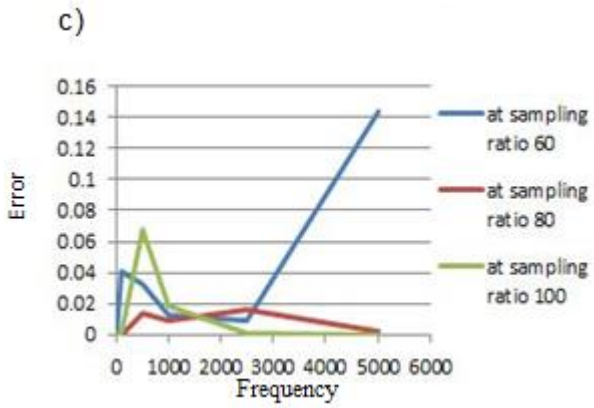
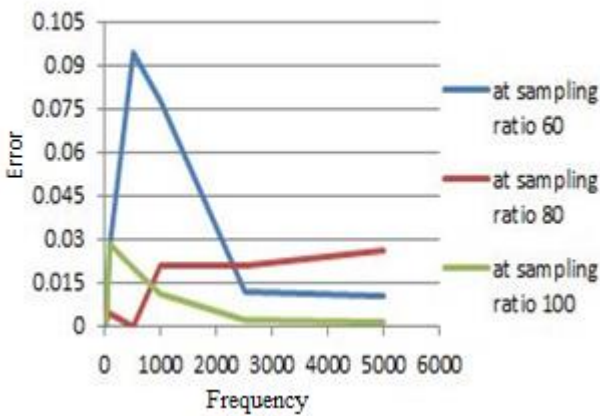
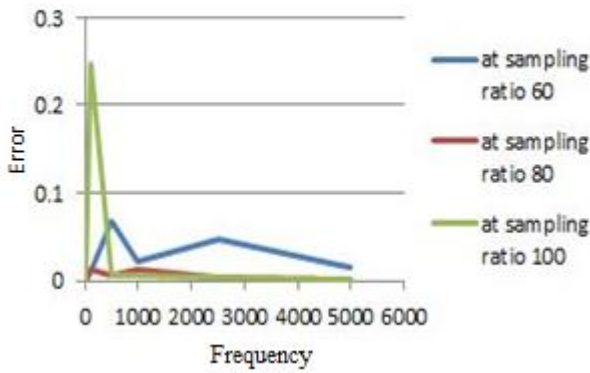


Fig. 4.16. Error in phase difference

a) Using 1 Volt, b) Using 3 Volts, c) Using 5 Volts



b)



c)

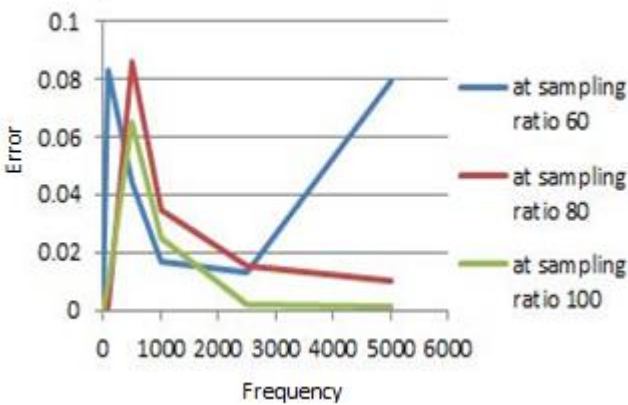


Fig. 4.17. Error in signal ratio

Using 1 Volt, b) Using 3 Volts, c) Using 5 Volts

The experimental results for the error in phase difference and signal ratio for different voltages 1 V, 3 V and 5V, and different sampling ratios 60, 80 and 100 are shown in Fig. 4.16. and Fig. 4.17.

Experiment 4 - The sample index are incremented by 1

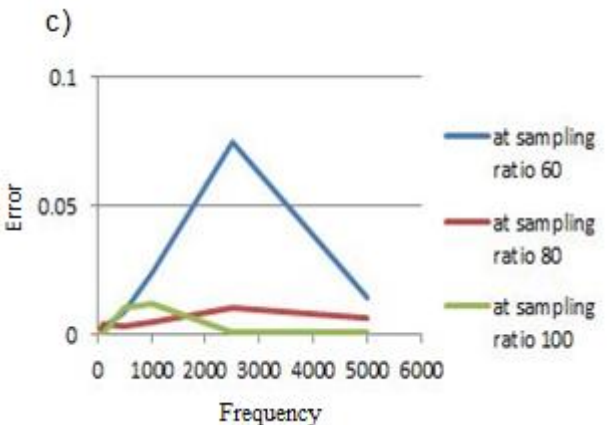
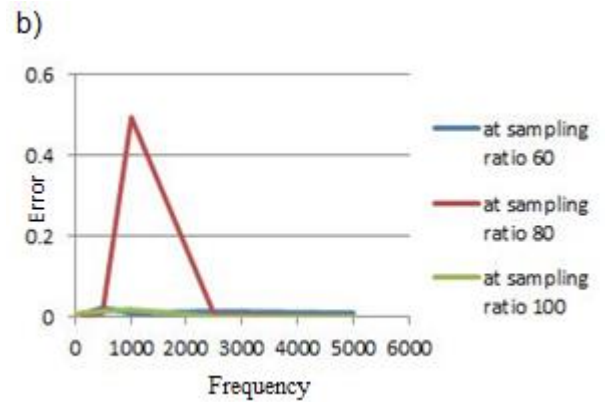
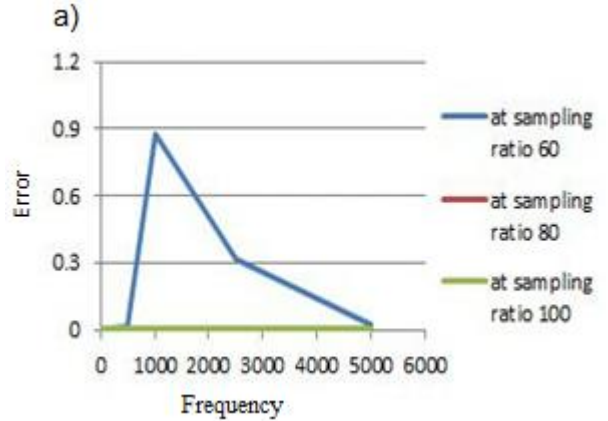
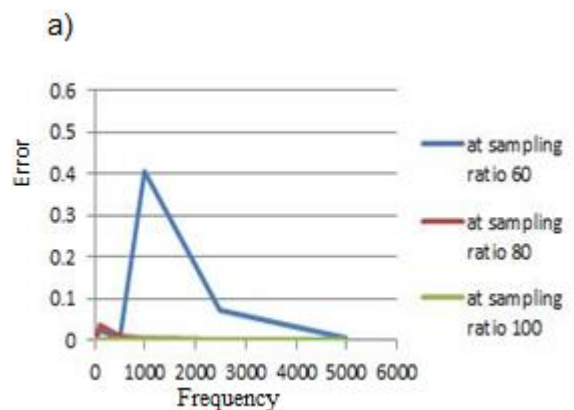


Fig. 4.18. Error in phase difference

a) Using 1 Volt, b) Using 3 Volts, c) Using 5 Volts



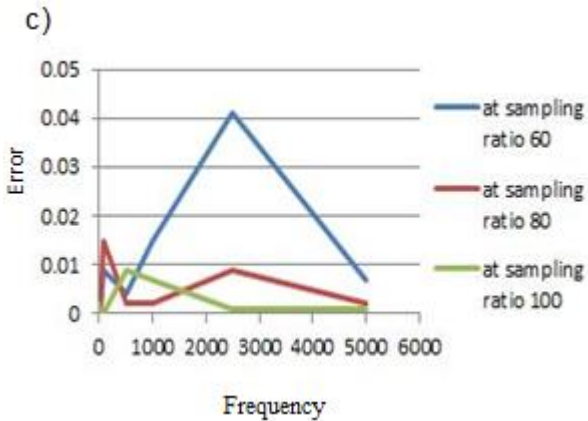
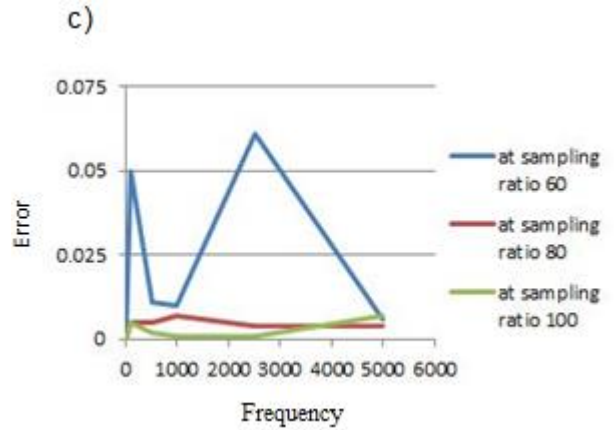
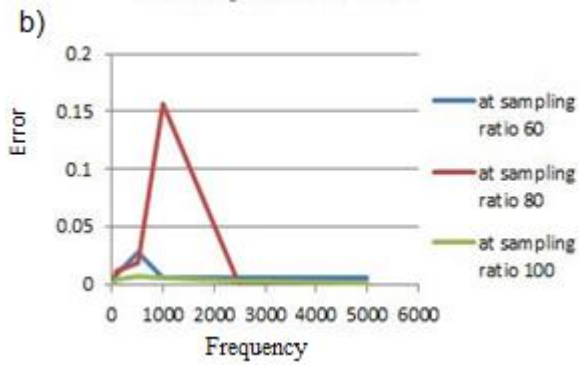


Fig.4.20. Error in phase difference
a) Using 1 Volt, b) Using 3 Volts, c) Using 5 Volts

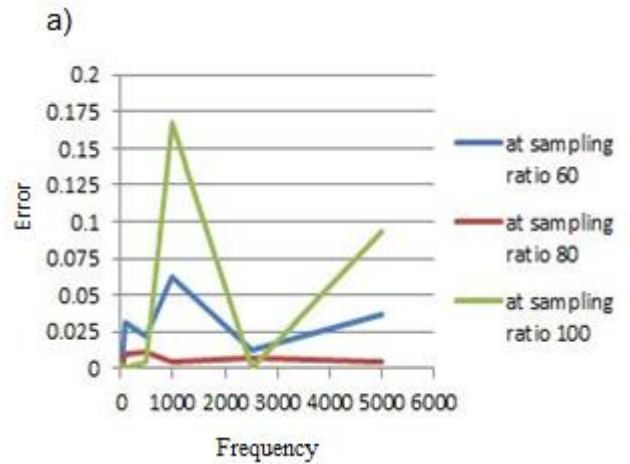
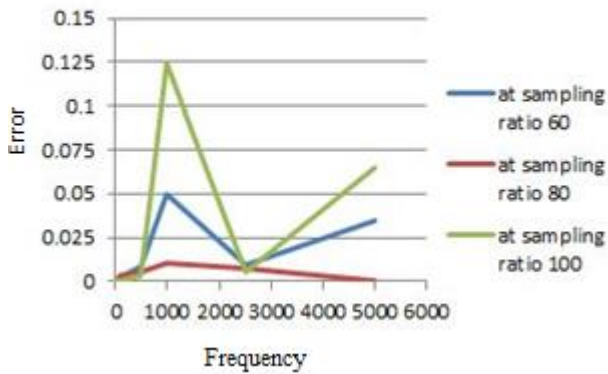
Fig. 4.19. Error in signal ratio

a) Using 1 Volt, b) Using 3 Volts, c) Using 5 Volts

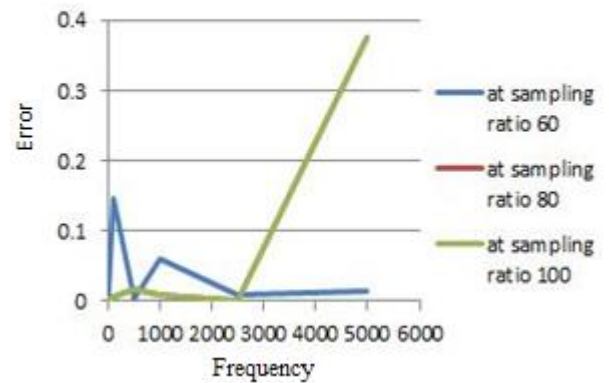
The experimental results for the error in phase difference and signal ratio for different voltages 1 V, 3 V and 5V, and different sampling ratios 60, 80 and 100 are shown in Fig. 4.18, and Fig. 4.19.

Experiment 5 - The sample index incremented by 3

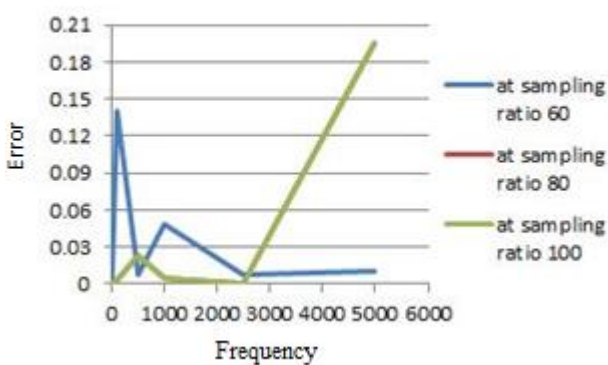
a)



b)



b)



c)

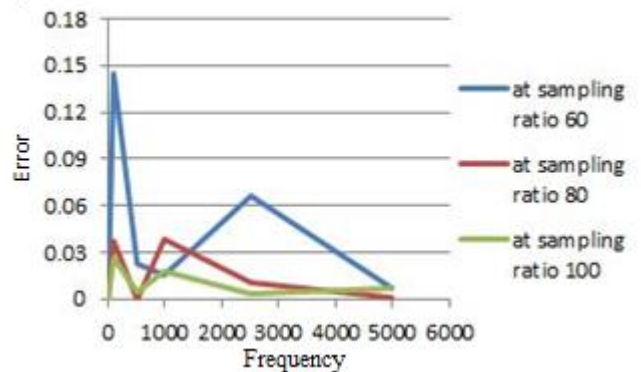


Fig.4.21. Error in signal ratio
a) Using 1 Volt, b) Using 3 Volts, c) Using 5 Volts

The experimental results for the error in phase difference and signal ratio for different voltages 1 V, 3 V and 5V, and different sampling ratios 60, 80 and 100 are shown in Fig. 4.20. and Fig. 4.21

V. RESULTS

It can be seen that, there are many advantages and disadvantages using particular sampling method over the most accepted DFT algorithms. As from the the experimental results of the particular sampling using the Lab-view application using DAQ card shows the main inference as that the error in computing the impedance is affected by the signal frequency and the voltage doesn't have any vast influence in the computation of the impedance

The mean value of error in computation of phase difference is plotted as a function of frequency is shown in Fig. 5.1. and it shows, increase in the frequency resulted in the error rate up to a certain extent

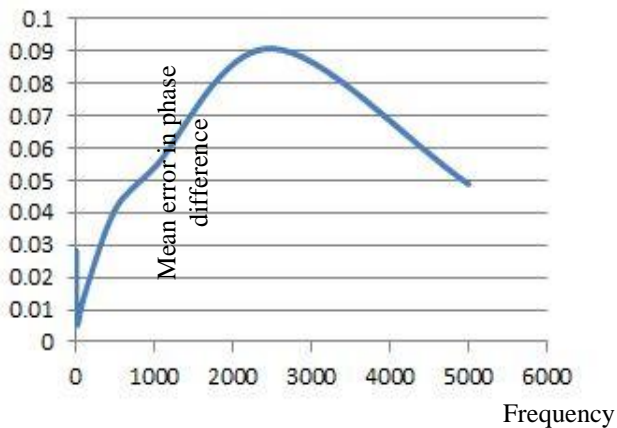


Fig. 5.1. Graphical result of value of error in phase difference

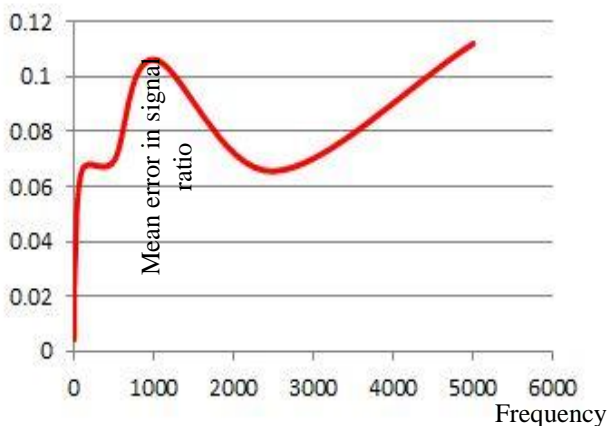


Fig. 5.2 . Result of mean value of error in signal ratio

The Fig. 5.2. shows the variation of the signal ratio error as a result of frequency change and it is evident from the graph that the errors increase with the increase in frequency.

The Fig. 5.3. shows the average percentage of error in computation of impedance using particular sampling method and it can be seen that the overall error in percentage varies from 2% in low frequencies to an average of 6% in high frequency.

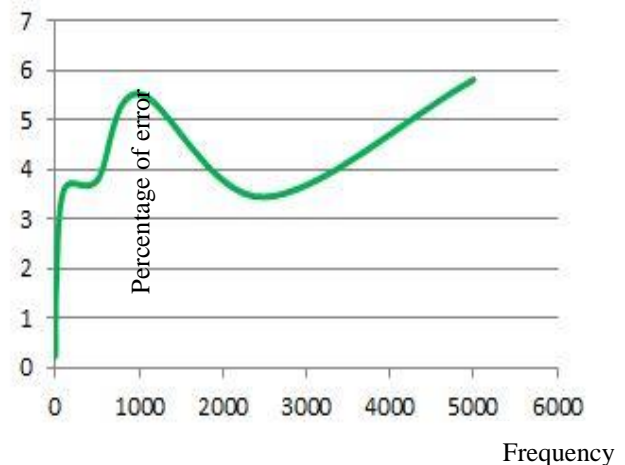


Fig. 5.3. Graphical result percentage of error for various frequencies

Advantages of particular sampling method

For N samples N^2 complex multiplications and $N(N-1)$ complex additions are needed for DFT algorithm So in our experiment (particular sampling takes minimum 60 samples). Total number of calculations using DFT will be 7140 complex multiplications and additions. For Particular sampling we need only additions and the total additions will be $4N$. So total calculations using particular sampling is 240

So when the time saving is considered, with the implementation of the particular sampling algorithm we will be saving a large amount of time and memory as the same for the same result as compared to DFT algorithm with a certain amount of error. As precisely there is saving of 96.3% time and memory if employ the particular sampling for the same purpose using DFT. As per the experimental results the maximum error in the calculation of impedance measurement is 6%.

It should be noted that the saving of time can be achieved in the loss of accuracy of the measurement with an average standard deviation of 0.041

VI. CONCLUSION

The use of the particular sampling method for impedance measurement allows to meaningfully decrease the number of samples and the calculation effort. For example, for the proposed realization only 8 samples for each part (Re, Im) of each signal (voltage, current) are acquired and then added. On the other side, the accuracy of the method as well as the immunity to noise is lower than in the DFT-based impedance measurement. The obtained accuracy is acceptable in case of measurement in the field and the resulting simplification of the device can open a new application area for impedance measurement (e.g. smart impedance sensors). The developed system is a prototype, which has made possible experimental verification of the method using particular sampling. The system has created a base for development of a simple, small impedance measuring application.

From the experimental results and comparing the DFT and particular sampling algorithms, it can be noted that DFT is more reliable and is accurate and more time consuming than the other methods. The memory needs to process a lot of mathematical data is more so it is the most possible disadvantage of DFT. While on the implementation of

particular sampling method we have a large saving of time and memory more than 90% and only a minute loss of accuracy of 6%. So the time is saved on expenditure of accuracy. The particular sampling methods provide an easy and not tiring method for impedance measurement and can be used for various domains of consumer application especially commercial.

REFERENCES

[1] R.N Jones, W.J Anson Meteorological Guide- The measurement of lumped parameter impedance, National bureau of standards, 17-129.
 [2] Zurich instruments. (2016), Principles of lock-in-detection and the state of the art, 1
 [3] Bradley Armen. G (2008) Phase sensitive detection Lock in amplifiers. 1-4.
 [4] Lentka, G. (2014) using a particular sampling method for impedance measurements, Metrology and Measurement Systems, vol XXI, no 3, pp. 497-508.
 [5] Hoja, J., Lentka G. (2011). Method using square-pulse excitation for high-impedance spectroscopy of anticorrosion coatings, *IEEE Transactions on Instrumentation and Measurement*, Vol. 60, 957–64.
 [6] Hoja, J., Lentka G. (2010). Interface circuit for impedance sensors using two specialized single chip Microsystems. *Sensors and Actuators A-physical*, Vol. 163, No. 1, 191–197.
 [7] Hoja, J., Lentka, G., Zielonko, R. (2002) Measurement microsystem for high impedance spectroscopy of anticorrosion coatings, *Metrology and Measurement Systems*, Vol. 9, No 1, 31–44.
 [8] Douglas L Jones. (2008), Decimation-in-Frequency (DIF) Radix-2 FFT, OpenStax-CNX module: m12018, 1-5.
 [9] Douglas L Jones. (2006), Goertzel's Algorithm, connexions module: m12024, 1-2.
 [10] Agilent technology, December 2003, impedance measurement handbook.
 [11] Ramos, P. M., Radil, T., Janeiro, F. M. (2012) Implementation of sine-fitting algorithms in systems with 32-bit floating point representation, *Measurement*, Vol. 45, No. 2, 155–163.
 [12] Ramos, P., Janeiro, F., Radil, T. (2010) Comparative Analysis of Three Algorithms for Two-Channel Common Frequency Sinewave Parameter Estimation: Ellipse Fit, Seven Parameter Sine Fit and Spectral Sinc Fit. *Metrology and Measurement Systems*. Vol. 17, Issue 2, pp. 255–270.
 [13] Ramos, P. M., Radil, T., Janeiro, F. M. (2012) Implementation of sine-fitting algorithms in systems with 32-bit floating point representation, *Measurement*, Vol. 45, No. 2, 155–163.
 [14] Smith, W. H. (1999) *The Scientist and Engineer’s Guide to Digital Signal Processing*, California Technical Publishing, San Diego, USA, 1999.
 [15] Cypress Semiconductor (2013) PSoC™ Mixed Signal Array Technical Reference Manual, Rev. H.
 [16] Pedro. M. R, Fernando. M. J, Tomas. R (2009). Comparison of impedance method in a DSP.
 [17] Phase sensitive detection, http://hades.mech.northwestern.edu/index.php/Phase-Sensitive_Detection (access date 8.11.2017).
 [18] DFT properties http://nptel.ac.in/courses/117104070/lecture6/slide_6_5.htm (access date 8.11.2017).
 [19] National Instruments USB-6251 Mass Term 16-Bit, 1.25 MS/s M Series Multifunction DAQ. https://www.artisanng.com/TestMeasurement/853731/National_Instruments_USB_6251_Mass_Term_16_Bit_1_25_MS_s_M_Series_Multifunction_DAO (access date 2.11.2017).

Fig. 2.8. Twin-T bridge
 Fig. 2.9. Q bridge
 Fig. 2.10. Thurston bridge
 Fig. 2.11. Young bridge
 Fig. 2.12. Series resonance a) Circuit
 Fig. 2.12. Series resonance b) Frequency response
 Fig. 2.13. Parallel resonance a) Circuit
 Fig. 2.14. Parallel resonance b) Frequency response
 Fig. 2.15. Q-meter
 Fig. 2.16. Immittance trans-comparator a) Circuit diagram
 Fig. 2.16. Immittance trans-comparator b) Frequency response
 Fig. 2.17. Vector impedance meter
 Fig. 2.18. L-C meter
 Fig. 3.1. Lock-in amplifier
 Fig. 3.2. Concept of lock-in amplifier
 Fig. 3.3. Phase sensitive detection
 Fig. 3.4. Schematic showing working of DFT
 Fig. 3.5. Computation of real and imaginary part using correlation
 Fig. 3.6. Acquired samples from two channels with (+) for channel 1 and (x) for channel 2 and the corresponding sine-fit reconstructed signals (lines).
 Fig. 3.7. Acquired samples from two channels (+) and the corresponding reconstructed ellipse (line)
 Fig. 3.8. Realization of Goertzel system
 Fig. 4.1. Error in magnitude estimation by DFT using matlab simulation
 Fig. 4.2. Error in phase determination using DFT by matlab simulation
 Fig. 4.3. Error in magnitude estimation by particular sampling using matlab simulation
 Fig. 4.4. Error in phase determination by particular sampling using matlab simulation
 Fig. 4.5. Noise amplitude versus the error in magnitude by DFT and particular sampling using matlab simulation
 Fig. 4.6. Noise amplitude versus the error in phase difference by DFT and particular sampling using matlab simulation
 Fig. 4.7. Block diagram and a view of prototype
 Fig. 4.8. Front Panel of labview application for signal generation
 Fig. 4.9. Front panel of labview application for sample acquisition
 Fig. 4.10. DAQ card NI USB - 6251 used for experiment
 Fig. 4.11. Circuit diagram showing experimental setup (DIPTRACE software)
 Fig. 4.12. Error in phase difference (experiment 1)
 Fig. 4.13. Error in signal ratio (experiment 1)
 Fig. 4.14. Error in phase difference (experiment 2)
 Fig. 4.15. Error in signal ratio (experiment 2)
 Fig. 4.16. Error in phase difference (experiment 3)
 Fig. 4.17. Error in signal ratio (experiment 3)
 Fig. 4.18. Error in phase difference (experiment 4)
 Fig. 4.19. Error in signal ratio (experiment 4)
 Fig. 4.20. Error in phase difference (experiment 5)
 Fig. 4.21. Error in signal ratio (experiment 5)
 Fig. 5.1. Graphical result of value of error in phase difference
 Fig. 5.2. Result of mean value of error in signal ratio
 Fig. 5.3. Graphical result percentage of error for various frequency

LIST OF TABLES

Table 3.1. Cost of calculation comparison of DFT and FFT
 Table 4.1. Example values and eliminated harmonics
 Table 4.2. Sampling schedule for the proposed particular sampling method implementation

LIST OF FIGURES

Fig. 2.1. Impedance vector analysis
 Fig. 2.2. Block diagram of the impedance measurement system
 Fig. 2.3. Wheatstone’s bridge
 Fig. 2.4. Maxwell’s bridge
 Fig. 2.5. Schering bridge
 Fig. 2.6. Admittance ratio bridge
 Fig. 2.7. Transformer bridge